NON-LINEAR EFFECTS IN A FOCUSED UNDERWATER ACOUSTIC SYSTEM

by

Kenneth Frank Scigulinsky

United States
Naval Postgraduate School

THESIS

NON-LINEAR EFFECTS IN A FOCUSED

UNDERWATER ACOUSTIC SYSTEM

by

Kenneth Frank Scigulinsky

December 1969

Non-Linear Effects in a Focused Underwater Acoustic System

by

Kenneth Frank Scigulinsky
Lieutenant, United States Navy
B.S.E.E., University of Washington, 1964

Submitted in partial fulfillment of the
requirements for the degree of

MASTER OF SCIENCE IN ENGINEERING ACOUSTICS

from the

NAVAL POSTGRADUATE SCHOOL
December 1969

ABSTRACT

A focused system having non-coincident foci was used to study the phenomenon of non-linear mixing in water. Primary frequencies of 343 kHz and 383 kHz provided a scattered difference frequency of 40 kHz. Enhancement of the difference frequency signal at incipient cavitation was verified. A delay between energization of the system and signal enhancement was linked to the state of non-linearity of the medium and provided strong evidence for the existance of a virtual source at 40 kHz. Directivity measurements of the focused system at 40 kHz revealed a multilobed structure, but the presence of pseudosound degraded the measurements and attempts to correlate the lobe structure with a particular virtual source configuration were unsuccessful.

TABLE OF CONTENTS

I. INTRODUCTION - 9

A. BACKGROUND - - - - - - - - - - - - - - - - - - - 9

B. OBJECTIVE - 10

II. THEORY FOR NON-LINEAR MIXING - - - - - - - - - - - - - 12

III. EQUIPMENT DESCRIPTION - - - - - - - - - - - - - - - - -15

A. TRANSDUCERS - - - - - - - - - - - - - - - - - - - 15

B. ELECTRONICS - - - - - - - - - - - - - - - - - - - 16

C. MECHANICAL - - - - - - - - - - - - - - - - - - - 18

IV. EXPERIMENTAL PROCEDURE; RESULTS - - - - - - - - - - - 19

A. GENERAL - 19

B. TRANSDUCER DIRECTIVITY - - - - - - - - - - - - - -19

C. ON-AXIS INTENSITY - - - - - - - - - - - - - - - - 20

D. LOCATION OF FOCUS - - - - - - - - - - - - - - - - 20

E. CAVITATION THRESHOLD - - - - - - - - - - - - - - - 21

1. Visual Determination - - - - - - - - - - - - 21

2. Subharmonic Detection - - - - - - - - - - - - 22

F. SPL AT FOCUS - - - - - - - - - - - - - - - - - - 23

G. DIFFERENCE FREQUENCY ENHANCEMENT - - - - - - - - - 23

H. SYSTEM DIRECTIONAL CHARACTERISTICS - - - - - - - - 23

I. PSEUDOSOUND EFFECTS - - - - - - - - - - - - - - - 24

J. TIME DEPENDENT EFFECTS - - - - - - - - - - - - - - 25

V. CONCLUSIONS - 27

APPENDIX A FIGURES - 30

BIBLIOGRAPHY - 54

INITIAL DISTRIBUTION LIST - - - - - - - - - - - - - - - - - 56

FORM DD 1473 - 57

LIST OF FIGURES

Figure 1 Transducer Mounting Details - - - - - - - - - - - - 30

Figure 2 Difference Frequency Probe - - - - - - - - - - - - -31

Figure 3 Probe Directivity at 40 kHz - - - - - - - - - - - - 32

Figure 4 System Block Diagram - - - - - - - - - - - - - - - -33

Figure 5 One Focusing Transducer and the Low Frequency Probe Mounted on the Rail - - - - - - - - 34

Figure 6 Focused System Mounted in the Rotation Jig - 34

Figure 7 Hemisphere's Radiation at 5.4 cm, 15V p-p, 383 kHz - - - - - - - - - - - - - - - - - -35

Figure 8 Hemisphere's Radiation at 10.8 cm, 15V p-p, 343 kHz - - - - - - - - - - - - - - - - - -36

Figure 9 On-axis SPL vs. Distance; 4V p-p, 383 kHz - - - - - - - - - - - - - - - - - - - 37

Figure 10 Transient Cavitation in Focal Region; 170V p-p, 383 kHz - - - - - - - - - - - - - - - - - 38

Figure 11 Cavitation Bubbles in Focal Region One Minute After Voltage was Applied - - - - - - - - -39

Figure 12 SPL at Focus vs. Drive - - - - - - - - - - - - - - -40

Figure 13 Difference Frequency Output vs. Primary Frequency Excitation -41

Figure 14 Typical Received Signal Prior to Filtering - - - -42

Figure 15 Radiated Difference Frequency; #1 = 4V; #2 = 15V - - - - - - - - - - - - - - - - - 43

Figure 16 Radiated Difference Frequency; #1 = 4V; #2 = 30V - - - - - - - - - - - - - - - - - - 44

Figure 17 Radiated Difference Frequency; #1 = 15V; #2 = 30V - - - - - - - - - - - - - - - - -45

Figure 18 Radiated Difference Frequency; #1 = 10V; #2 = 10V - - - - - - - - - - - - - - - - - -46

Figure 19 Radiated Difference Frequency;
#1 = 10V; #2 = 10V; 8° to 92° - - - - - - - - - - - 47

Figure 20 SPL vs. Bearing for 383 kHz - - - - - - - - - - - - 48

Figure 21 SPL vs. Bearing for 343 kHz - - - - - - - - - - - - 49

Figure 22 Ray Geometry for Source at Focus - - - - - - - - -50

Figure 23 Difference Frequency vs. Time;
#1 = 40V; #2 = 4V; #1 = 30V; #2 = 4V - - - - - - - -51

Figure 24 Difference Frequency vs. Time;
#1 = 75V; #2 - 20V - - - - - - - - - - - - - - - - - -52

Figure 25 Difference Frequency vs. Time;
#1 = 83V; #2 = 20V - - - - - - - - - - - - - - - - - -53

ACKNOWLEDGEMENT

The author wishes to acknowledge the support and encouragement provided him by Professor Donald A. Stentz. His optimistic guidance in pursuing alternate approaches to problems created by equipment deficiencies made this thesis possible. In addition, the author commends the imaginative efforts of machinists Robert Moeller and Thomas Maris. Their ability to quickly convert a verbally expressed idea into a finished product that would do the job was a most welcome service.

I. INTRODUCTION

A. BACKGROUND

Two or more sound waves passing through a common region in a fluid will experience an interaction. This coupling effect is due to the non-linear terms in the wave equation and one of the results is a scattered wave. The frequency of the scattered wave is determined by the frequencies of the interacting waves.

By utilizing Lighthill's equation of aerodynamically generated sound [1], Westervelt was able to mathematically analyze the effect of two sound waves passing through a common region in a perfect fluid [2].

When considering only the lowest order scattering process, he obtained a source function which was quadratic in the primary field variables. The solution of the resulting wave equation for the plane wave case showed that no combination waves should be scattered outside the region transversed by two perfectly collimated plane waves forming a non-zero angle between them. Westervelt's work was corroborated when experiments by Bellin and Beyer [3],and Muir and Blue [4] showed little deviation with his plane wave scattering theory.

The solutions for the interaction of two concentric cylindrical waves and of two concentric spherical waves was presented by Dean [5], while the case of eccentric cylindrical and spherical sources was treated by Lauvstad [6].

An experimental investigation by Dunn, Kuljis and Welsby [7] was directed, in part, towards studying the scattered sound from a region having pressures bounding the cavitation region. To obtain high acoustic intensities with only moderate power, they used a roughly

focused system comprised of two spherically concave transducers having coincident foci.

One transducer was driven at 326 kHz at constant voltage, while the other transducer was driven at 373 kHz and its voltage varied. They found that when the level of fixed excitation was sufficient to cause cavitation, the signal created at the difference frequency (47 kHz) rose smoothly to a plateau as the variable excitation was increased; however, when the fixed excitation was insufficient to induce cavitation, increasing the variable excitation resulted in a very slight increase in signal level up to the cavitation threshold. Beyond the threshold the signal level rose rapidly, attaining the same plateau as in the first case. One of their conclusions was that the interaction of standing wave fields at two different primary frequencies can produce a virtual source of radiated energy at the difference frequency, and that although cavitation increases the effect, it is not necessary.

B. OBJECTIVE

Since only a limited amount of experimental data on focused systems was available, a logical first step in entering this experimental area was to confirm some of the previously obtained results. Once this was accomplished, the goal was to study some of the phenomena which were observed by earlier researchers, but which had received little attention.

The work of Dunn, Kuljis and Welsby alluded to the directional characteristics of the focused field, but this aspect of a focused system was not studied in detail; therefore, it was decided to investigate the directional field of a focused system having non-coincident

foci and determine to what extent a virtual source of the difference frequency is created. Additionally, some quantitative measures of the time dependence of the scattered difference frequency was desired.

II. THEORY FOR NON-LINEAR MIXING

When the wave equation is normally derived, approximations are made which are tenable because of the low amplitude signals usually encountered in acoustics work. One example of such an approximation involves the Acoustic Continuity Equation:

$$\nabla \cdot (\rho \bar{v}) + \frac{\partial \rho}{\partial t} = 0 \qquad (1)$$

$\rho = \rho_0 + \rho_1$ is the instantaneous total fluid density of a small region

ρ_0 = ambient density

ρ_1 = acoustic density

$\bar{v}$ = the instantaneous vector particle velocity

When equation (1) has been expanded the following approximations may be made:

$$\frac{\rho_1}{\rho_0} \cong \frac{\rho_1}{\rho_0} << 1$$

$$\nabla p_0 = \nabla \rho_0 = \frac{\partial \rho_0}{\partial t} = 0$$

$p = p_0 + p_1$ is the instantaneous total field pressure at a point in the medium

p_0 = ambient pressure

p_1 = acoustic pressure

With these approximations, equation (1) simplifies to:

$$\rho_0 \nabla \cdot \bar{v} + \frac{\partial \rho_1}{\partial t} = 0 \qquad (2)$$

When this result is coupled with the assumption of adiabatic reversibility for an acoustic wave, the resulting wave equation, equation (3), represents a linear system. By linear is meant that the system parameters are independent of the amplitude of excitation; therefore, the Superposition Theorem applies when two or more sinusoidal waves of different frequency exist in the medium.

$$\frac{\partial^2 p_1}{\partial t^2} = \frac{\kappa_0}{\rho_0} \nabla^2 p_1 \qquad (3)$$

κ_0 = bulk modulus for a static fluid

$\sqrt{\kappa_0/\rho_0}$ = velocity of propagation

When waves of high intensity are generated, the previous approximations are invalid, and the ratio κ_0/ρ_0 in equation (3) should be replaced by a function κ/ρ which is a function of acoustic pressure [8].

$$\kappa/\rho = \kappa_0/\rho_0 \left(1 + a_1 p + a_2 p^2 + \ldots\right) \qquad (4)$$

where a_1, a_2, ... are constants determined by the parameters of the fluid

When this substitution is made, the time-space relationship of the pressure waveform becomes dependent upon a velocity of propagation which is, at any point, a function of the instantaneous pressure at that point. This non-linear effect will cause two sinusoidal waves of frequencies f_1 and f_2 to interact, generating frequencies $nf_1 + mf_2$. Here n takes on all integral values from 0 to ∞, and m takes on all integral values from $-\infty$ to $+\infty$. While this approach is very general, it expresses the concept of non-linear mixing.

Westervelt's precise approach was based upon a calculation of the scattered pressure field due to non-linearities within a small interaction volume [2]. Discounting any distortion of these second-order effects as they propagate in a non-linear manner, he obtained an inhomogeneous wave equation for the acoustic density of the scattered wave:

$$\Box^2 \rho_s = c_o^{-2}\left\{\Box^2 E - \nabla^2\left[2T + \rho_o c_o^{-2}\left(\frac{d^2 p}{d\rho^2}\right)_{\rho=\rho_o} V\right]\right\} \quad (5)$$

T = Kinetic energy density = $\frac{1}{2}\rho_o u^2$

V = Potential energy density = $\frac{1}{2}c_o^2 \rho_o^{-1} \rho^2$

E = Total energy density = $T + V$

c_o = Velocity of sound

ρ_s = Acoustic density of the scattered wave

u = Instantaneous particle velocity

The theoretical extension of Westervelt's work to cylindrical and spherical spreading waves was accomplished by Lauvstad [6] and Dean [5], but the theoretical analysis of interactions within a focused, standing wave system has, as yet, not been accomplished. Because of the lack of a theoretical model, measurements and observations associated with this research could only be compared to experimental work done by others. It was expected though, that sufficient observations would spark some theoretical opinions, expressed as extensions of the approaches discussed above.

III. EXPERIMENT DESCRIPTION

A. TRANSDUCERS

The transducers chosen for the focused system were three inch diameter lead zirconate-titanate hemispheres, having a resonant frequency of 355 kHz when operated in the thickness made. The hemisphere was chosen in lieu of a portion of a hemisphere because it was anticipated that the driving voltage to the system would be limited by available equipment. The additional surface area, therefore, was needed to reduce the voltage required to achieve the desired cavitation condition. This decision immediately precluded the possibility of studying a focused system with coincident foci since the focus for a hemisphere does not occur at an on-axis distance from the surface which is greater than the radius of curvature [9].

Mountings for the transducers were constructed from aluminum cylinders, and the transducers were held in place with epoxy, which also acted as a seal. The construction details are shown in figure 1. After the transducer housing was completely assembled, conducting silver paint was applied around the inner perimeter of the transducer so that a continuous conducting strip bridged the plastic insulator and contacted the aluminum housing. While the paint was still tacky, narrow strips of aluminum foil were pressed into the paint, over-lapping the edges of the plastic insulator. This was done to insure that an adequate current path from the transducer face to the aluminum housing would be formed. The aluminum housing provided the return or ground side of the circuit. Finally, the complete unit was coated with epoxy and then liquid neoprene. Although the transducers had similar characteristics

they were numbered 1 and 2 so that control could be maintained. Further reference to transducer 1 or transducer 2 will be abbreviated #1 or #2, and the term "transducer" will be used to mean the complete unit shown in figure 1. All distances from a transducer are measured from the mounting face, unless otherwise specified.

Two different probes were used, one for measurements at the relatively high primary frequencies (343 kHz and 383 kHz), and one for the relatively low frequency (40 kHz) difference wave. The active element of the high frequency probe was a 1/8" square piece of barium titanate mounted on a 1/8" diameter tube. The low frequency probe utilized an Atlantic Research LC-65 pressure transducer mounted in a brass housing (see figure 2). For the frequencies measured, the probe used was smaller than a wavelength in water (λ = 0.392 cm at 383 kHz and λ = 3.77 cm at 40 kHz). Both probes were calibrated by the method of substitution [10] using calibrated LC-32 and USN standard type E-8 hydrophones. The sensitivities of the transducers were as follows:

DIFFERENCE, OR LOW FREQUENCY PROBE	-91 dB re 1V/μbar at 40 kHz
PRIMARY, OR	-102 dB re 1V/μbar at 343 kHz
HIGH FREQUENCY PROBE	-96.2 dB re 1V/μbar at 383 kHz

The directivity plot for the low frequency probe, figure 3, shows that the beamwidth, based upon the -3 dB points, is at least 30°. The high frequency probe was essentially omnidirectional.

B. ELECTRONICS

The following types of equipment were used in the investigation:

Item	Model
SIGNAL GENERATOR	HP 650A
FREQUENCY COUNTER	HP 5232A

OSCILLOSCOPE	TEKTRONIX 515A
VOLTAGE AMPLIFIER	HP 450A
POWER AMPLIFIER	GR 1233A
WAVE ANALYZER	GR 1900A
*WAVE ANALYZER	HP 3590A
RADIO TRANSMITTER	TDE-3 (navy model)
VTVM	HP 400C
X - Y PLOTTER	HONEYWELL 320

*was not available until late in the investigation

The TDE -3 is a military transmitter capable of producing 125 watts in the CW mode. Because it was designed for communications purposes, it was not possible to drive a transducer for longer than 30 seconds without risking damage to the transmitter. This restriction limited the use of the transmitter to investigations requiring short observation.

Measurements made with the GR 1900A were over a 50 Hz bandwidth, and the meter response time was set at either fast (0.15 second), or medium (0.5 second). The 99% confidence limits[#] for the meter speeds are:

Fast	-2.5 to +3.3 dB
Medium	-1.4 to +1.7 dB

Because the signal generators used had a tendency to drift, all measurements were made using AFC.

[#]One chance in 100 that the ratio of the long time average value to a selected meter reading will be beyond the range shown.

C. MECHANICAL

A set of rails with two moveable slides was used to position the probes. A special holder, constructed in two halves, allowed the probes or transducers to be positioned and then rotated to fixed angular positions. Figure 5 shows one transducer and the low frequency probe installed on the rail.

To investigate the directional properties of the focused system, it was considered easier to rotate the focused system than to move the probe to various angular positions. A jig was constructed which allowed the focused system to be rotated approximately 90° for a 7 cm transducer separation. Figure 6 shows the focused system in the jig.

IV. EXPERIMENTAL PROCEDURE; RESULTS

A. GENERAL

Originally the investigation was to have been carried out in a 2' x 4' x 6' plywood tank lined with one inch of rubberized hair; but, because initial measurements showed that standing waves were present, a 6' x 8' x 24' anechoic tank was used instead.

The mechanical resonance of each transducer was determined by finding the frequency which maximized the output under the condition of constant voltage input [11]. This value was found to be 355 kHz for each transducer. Equipment limitations prevented analyzing a difference frequency of greater than 50 kHz, and so a 40 kHz difference was decided upon. The choice of the primary frequencies was made by examining the loaded output of the TDE - 3 for various frequencies and noting those which minimized the VSWR on the connecting coaxial cable. The most acceptable VSWR, 1.1: 1, was realized at 343 kHz and so the TDE - 3 was used at this frequency while the drive at 383 kHz was achieved through the arrangement shown in figure 4.

Because this investigation was concerned with the interaction of acoustic fields, it was important to know the directional characteristics of each transducer.

B. TRANSDUCER DIRECTIVITY

Transducer #1 was driven with a 15V p-p, 383 kHz signal, and the high frequency probe was located at 5.4 cm from the transducer. The transducer was then rotated about its support, and the directional pattern shown in figure 7 was obtained. A second directional pattern was obtained at 343 kHz with the probe at 10.8 cm from the transducer (see

figure 8). An attempt to repeat the directional measurements at drive levels producing cavitation was unsuccessful because of large noise-like fluctuations.

C. ON-AXIS INTENSITY

O'Neil's theory predicting the on-axis intensity for a spherical focusing radiator is not valid for a hemisphere because one requisite is that the radius of the circular boundary of the spherical cap be large relative to the depth of the concave surface [9]; therefore, it was decided to probe the on-axis near-field to get a rough estimate of the relative intensity. The on-axis plots were similar for both primary frequencies, and figure 9 shows the plot for #2 at 383 kHz as a representative result. For the same driving voltage, the level of the signal at 343 kHz was greater than at 383 kHz. This result was expected though, since operation near resonance is more efficient.

D. LOCATION OF FOCUS

Theory predicts that, for a hemisphere, the focus will be located at the same point as the center of curvature. This was verified by placing transducer #1 in a 14 cm x 19 cm x 28 cm plexiglass tank and then driving it at 343 kHz with a 170V p-p signal. This level of drive was sufficient to achieve transient cavitation [12]. Attendant with this effect was sporadic acoustic streaming which carried cavitation bubbles through the focal region, allowing visual observation of both the convergence and the divergence around the focus. The effect was intermittent, and hence it was difficult to record on a photograph. Figure 10 shows the micro-bubbles in the focal region just before foggy streaming [13] commenced. A measurement of the on-axis location of the focus confirmed the fact that it was within 0.1 cm of the center of curvature of the hemisphere.

E. CAVITATION THRESHOLD

1. Visual Determination

Because of the presence of small cavitation bubbles between the focused transducers enhances the level of the scattered difference frequency, it was necessary to have a rough estimate of the driving voltage required to achieve cavitation. This was accomplished by focusing the two transducers and then placing the focused system in the plastic water tank. Future references to the focused system shall be interpreted to mean the two transducers with parallel faces, separated by 7.0 cm. For the test, #1 was operated at 343 kHz and #2 at 383 kHz. The driving voltage applied to #2 was kept at zero while the driving voltage to #1 was increased from zero in 5V steps. At 35V p-p, small bubbles were seen in the vicinity of the focus of #1 and after a 5 minute wait bubbles were found to be fairly uniformly distributed between the two transducers. Some of the bubbles were seen to vibrate, both horizontally and vertically. While the predominant motion was vertical (due to buoyant forces), some short horizontal movements were witnessed, both with and without coalescence. Of particular interest was the observation that within the space separating the two transducers, the vertical bubble motion occurred in discrete jumps between visually undefined layers.

When the voltage to #1 was reduced to zero, it was found that incipient cavitation occurred when the voltage to #2 was 30V p-p. Figure 11 shows some of the bubbles in the vicinity of the focus of #2 one minute after driving voltage was applied.

To ascertain whether the voltage applied to one of the transducers in the focused system would influence the cavitation-voltage threshold of the other transducer, various combinations of driving voltage were tried. The following table summarizes the results and shows that the

cavitation-voltage threshold for one transducer in a focused system is strongly influenced by the voltage applied to the other transducer.

Transducer #1 @ 343 kHz Volts p-p	Transducer #2 @ 383 kHz Volts p-p	Cavitation at focus of #1	Cavitation at focus of #2
30	0	no	no
35	0	yes	no
0	25	no	no
0	35	no	yes
10	30	yes	yes
15	30	yes	yes
25	30	yes	yes
25	4	no	no
25	15	no	yes

2. Subharmonic Detection

Late in the conduction of the investigation a wave analyzer with the capability to analyze high frequencies was received and so it was used to recheck the cavitation-voltage threshold by the method of subharmonic detection [14]. The system was focused and the high frequency probe was placed at the focus of #1. The probe output went directly to the wave analyzer which was tuned to one-half of the driving frequency (1st subharmonic) of #1. No voltage was applied to #2 during this part of the test. The drive to #1 was increased until the subharmonic was detected. This procedure was carried out for #1 and #2 at both primary frequencies with the following results:

	Cavitation-voltage threshold at 343 kHz	Cavitation-voltage threshold at 383 kHz
Transducer 1	18V p-p	22V p-p
Transducer 2	14V p-p	18V p-p

Subharmonic generation is acknowledged to be the most accurate indication of incipient cavitation because bubbles, if visible at all, do not

occur immediately when the threshold is reached. For this reason the values obtained by subharmonic detection were accepted as the voltage threshold.

F. SPL AT FOCUS

An attempt was made to measure the sound pressure level (SPL) of the primary frequencies at the focus of each transducer while the system was focused. Figure 12 shows the plot of SPL vs Driving Voltage for each transducer at each primary frequency. The accuracy of these values is questionable since the presence of the probe alters the field configuration and eliminates the central portion of the focus; nevertheless, the curves provide some useful information since the shapes still reveal the relationship between driving voltage and SPL.

G. DIFFERENCE FREQUENCY ENHANCEMENT

Prior to the actual investigation of the directional pattern of the focused system, it was decided to measure the SPL of the difference frequency to confirm that the system actually did behave as reported by Dunn, Kuljis and Welsby [7]. The transducers were focused and the probe was placed at 11 cm along the perpendicular bisector of the system axis (defined by a line connecting the centers of the two hemispheres). The driving voltage to #1 was varied from 4V p-p to 50V p-p while the voltage to #2 was kept constant. Five such runs were made using constant values of 4, 8, 15, 25 and 30V p-p. The results, shown in figure 13, indicate that signal enhancement does occur when the cavitation region is reached. Figure 14 shows the form of the received signal prior to filtering.

H. SYSTEM DIRECTIONAL CHARACTERISTICS

The directional characteristics of the scattered difference frequency were investigated by mounting the focused system in the rotatable jig

(figure 6) and making measurements at a distance of 66 cm. The total angular rotation of the jig was limited to about 90° because of interference between the pivot support bar and the transducer support stems. Figures 15 - 18 show the radiation pattern over the range 318° to 48° for various combinations of driving voltage. The appearance of incomplete large lobes at the extremes of the angular rotation of the jig led to an attempt to complete the lobe data. Unfortunately, when the system was readjusted to study the lobe at 048°, the orientation of the individual transducers shifted and the original pattern could not be reconstructed (see figure 18). One puzzling outgrowth of the attempt was the occurrence of a portion of a major lobe at 090°.

I. PSEUDOSOUND EFFECTS

The possibility that pseudosound (non-linear mixing of the primary frequencies at the probe) was being mistaken for the scattered difference frequency was considered. One brief experiment with SOAB (a B. F. Goodrich Co. rubber having selective frequency absorptive properties) to determine the source of the difference frequency was unsuccessful because the attenuation of the primary and difference frequencies were similar. A second attempt to isolate the source of the 40 kHz signal involved comparing the strength of the difference frequency while the system was focused with that measured when both transducers were pointing at the probe. If pseudosound was the source of the difference frequency, then the latter situation should have maximized the 40 kHz signal. The results tended to discount the effects of psuedosound since the received signal for the focused condition produced signals which were from 2 to 20 dB greater than for the unfocused configuration (the larger driving voltages produced larger differences). Trying another approach, the HP

359A wave analyzer was used to obtain the focused system's directivity pattern at each primary frequency while the system was being driven (figures 20 and 21). The peaks and dips on the plot were interpreted as an interference effect due to direct radiated waves from a transducer combining (at the probe) with waves reflected from the other transducer. The results only tended to strengthen the case for psudosound since the SPL's of the primary frequencies were generally above the SPL of the difference frequency. For example, calculations for the conditions existing when figure 19 was plotted show that the following readings occur within $\pm 2°$ of 090°.

SPL = 10.2 dB for 383 kHz at 90°
SPL = 30.5 dB for 343 kHz at 88°
SPL = 0.0 dB for 40 kHz at 92°

Having found no way to discern between scattered sound and psuedosound, attention was returned to interpreting figures 15 through 18. The large lobes at 318° and 048° strongly suggested that the wave interaction was taking place primarily at the foci, creating two virtual sources. The system geometry seemed to suggest that partial shielding of these sources was influencing the directivity. Figure 22 shows the system geometry and includes some limiting ray paths, assuming point sources at the two foci. While it appeared,at first, that the measured directivity patterns could be explained by two virtual sources at the foci, the explanation was clouded by many unknowns. The strength and phase relationship of the virtual sources was not known. More important, the physical size of the virtual sources was unknown.

J. TIME DEPENDENT EFFECTS

The time dependence of SPL measurements was obvious throughout the experiment. Although it was easy to rationalize the variation of

measurements over long periods of time as being caused by reflections from large bubbles, the short term fluctuations required further investigation.

The low frequency probe was placed 14 cm from the center of the focused system, at an angular position of 318° and was aimed at the focus of transducer #1. The probe output was filtered, and the 40 kHz component was converted to d.c. to drive the x-y plotter, thus recording the difference frequency voltage level vs. time. Figures 23 to 25 show the SPL versus time, for four combinations of driving voltage. Figure 23 indicates that there is a definite time delay between the application of the system voltages and the enhancement of the difference frequency. Figures 24 and 25 reveal that higher driving voltages eliminate the delay time but seem to produce an overshoot of the final average value. Visual observation did not allow complete correlation of signal level and bubble activity, but the absence of any visible bubbles during the first couple of seconds after turn-on seem to allow the following interpretations of figure 24.

The system is energized at time t_o and cavitation nuclei begin growing, thus increasing the compressibility of the water. This non-linear action increases until time t_1, when bubble growth and coalescence begin to outweigh the creation of new cavities. As this process continues, the radiation resistance of the medium decreases and the radiated power is reduced [15]. At time t_2 a fairly stable condition is reached with signal fluctuation being caused by:

1) Interference effects, due to energy scattered by the bubbles combining out of phase with the virtual sources.

2) Bubbles screening a portion of the interaction region, thereby altering the virtual sources.

3) The absorption of energy by the bubbles.

V. CONCLUSIONS

The directivity plot for the difference frequency in a focused system was found to have a multilobed structure. While the magnitude of the driving voltages altered the angular position of the lobes very little, the size of the lobes changed unpredictably. Increasing the distance at which measurements were made shifted the lobes a few degrees, indicating that interference effects might be responsible for the lobe structure.

Attempts to relate the lobe structure to some virtual source configuration in the interaction region were inconclusive. Although it was suspected that the virtual source would occupy a large portion of the volume between the transducers, it seemed likely that the energy density of the source would be greatest around the two foci. If this were true, then the shape of the radiation pattern should have been dominated by the effect of these "point" sources. Furthermore, ray theory showed that the major lobes should appear somewhere between 322° and 038°. Probing of the field, however, showed the major lobe in the first quadrant occurred at about 090°, a location where the difference frequency signal was expected to be smallest. A follow-up comparison of the difference frequency SPL with that of the primary frequencies over the positions from 15° to 95° indicated that the SPL at the difference frequency was always 10 to 35 dB lower than the SPL for either primary frequency. With such large differences, pseudosound was a possibility which could not be dismissed.

In spite of the possible effects of psuedosound, the case for a dominant "point" source was supported by the evidence that for a given position the response of the probe to the difference frequency could be maximized by aiming the probe face at the focus of the transducer with the largest driving voltage.

Future experiments should consider the presence of pseudosound and utilize techniques to circumvent or isolate its effects. One method might be to make directivity measurements using two probes having different nonlinear characteristics and then use a correlation technique to separate the pseudosound from the scattered sound.

The relative positions of the two transducers in the focused system are critical and therefore apparatus which allows acoustic measurements to be made without disturbing the system is needed. Specifically, the directional characteristics for 360° around the system should be obtainable without moving the focused system. This means that accurate positioning of a probe around the system is necessary. Additionally, the relative positions of the transducers should be controllable to about $\pm$1mm. Such accuracy would allow an analysis of the effect of transducer spacing and position upon the scattered difference frequency.

The repeatability of acoustic measurements made during cavitation is very poor because the cavitation bubbles mask, scatter, and absorb energy in a random manner.

Time recordings of the difference frequency signal show that the mechanism responsible for signal enhancement is not activated immediately after the system is energized. Using the drive combination of 4V p-p and 30V p-p at the primary frequencies, enhancement was not effective until 8 seconds after turn on. The delay was reduced to about 1 second when the driving combination was increased to 20V p-p and 75V p-p. This phenomenon invites a study of the time history of cavitation bubbles, using a high speed sequence camera. Such a study could shed more light on the precise conditions required for signal enhancement.

The proof, then, that non-linear mixing was actually achieved within the medium is supported by the fact that it was possible to influence the generation of non-linear conditions in the medium. By controlling the time-rate-of-growth of the non-linearity, the enhancement of the difference frequency was similarly controlled. Positive proof of non-linear mixing will exist only after further research confirms that large increases in the SPL of the primary frequencies do not occur concurrently with the creation of the non-linearity.

While the focused system currently has no practical applications, it is invaluable as a research tool for studying non-linear acoustic phenomena as well as cavitation effects. Perhaps future work can incorporate the use of optical diffraction to determine the configuration of the virtual source.

Lastly, a measure of the efficiency of the virtual source is needed. If it turns out to be as inefficient as for plane wave mixing [16], then the application of a focused system may depend solely upon its directional properties.

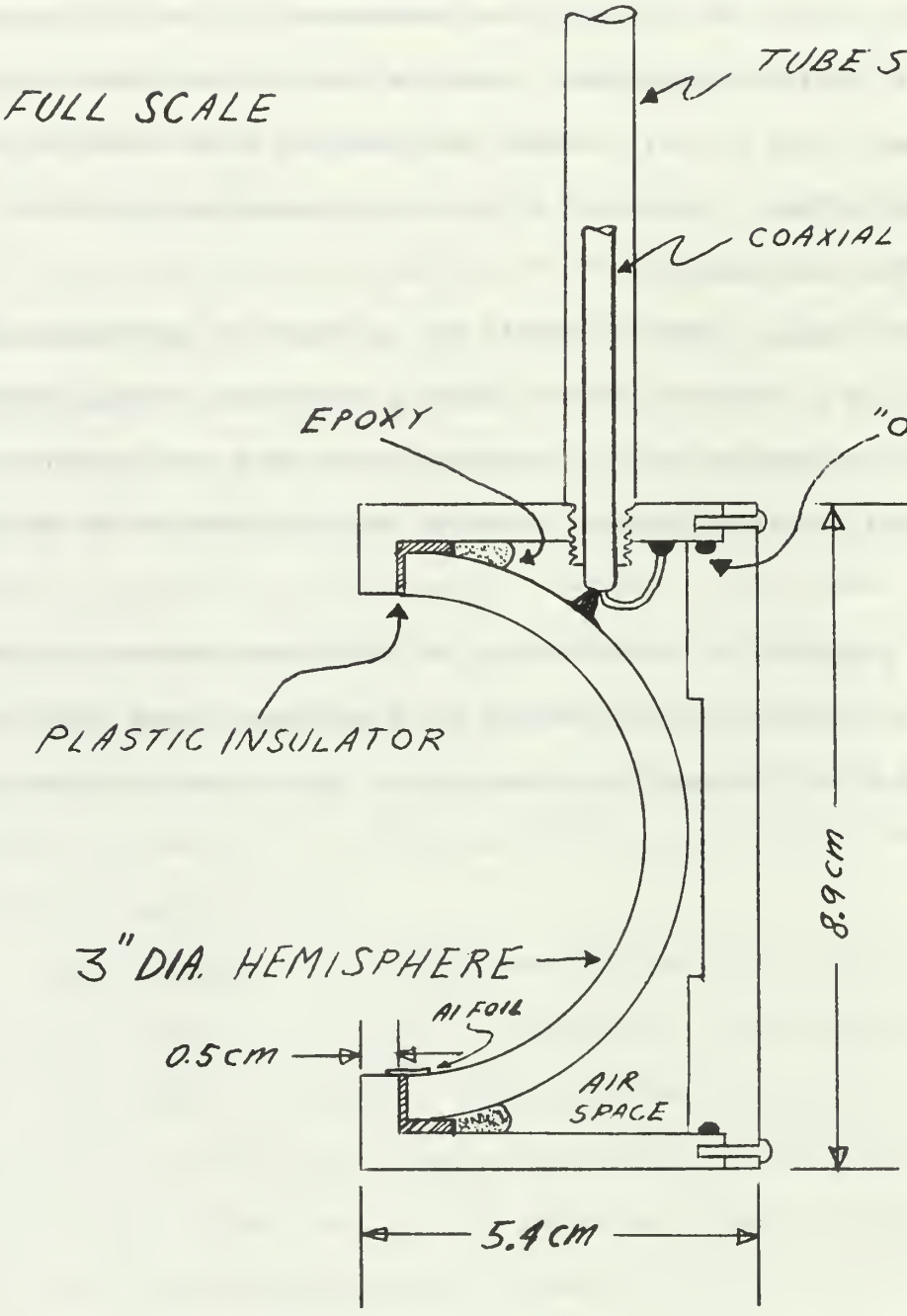

TRANSDUCER MOUNTING DETAILS

FIGURE 1

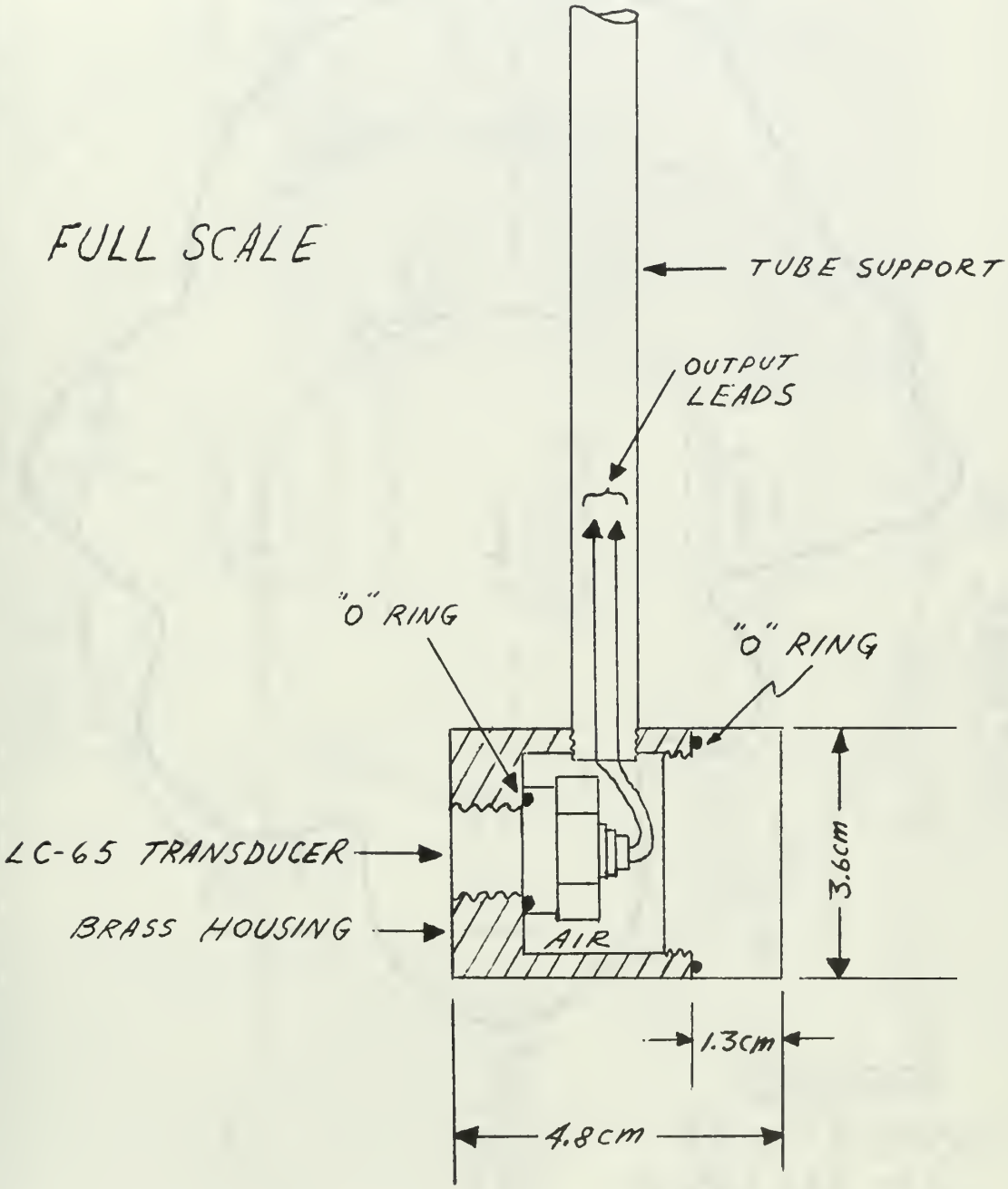

DIFFERENCE FREQUENCY PROBE

FIGURE 2

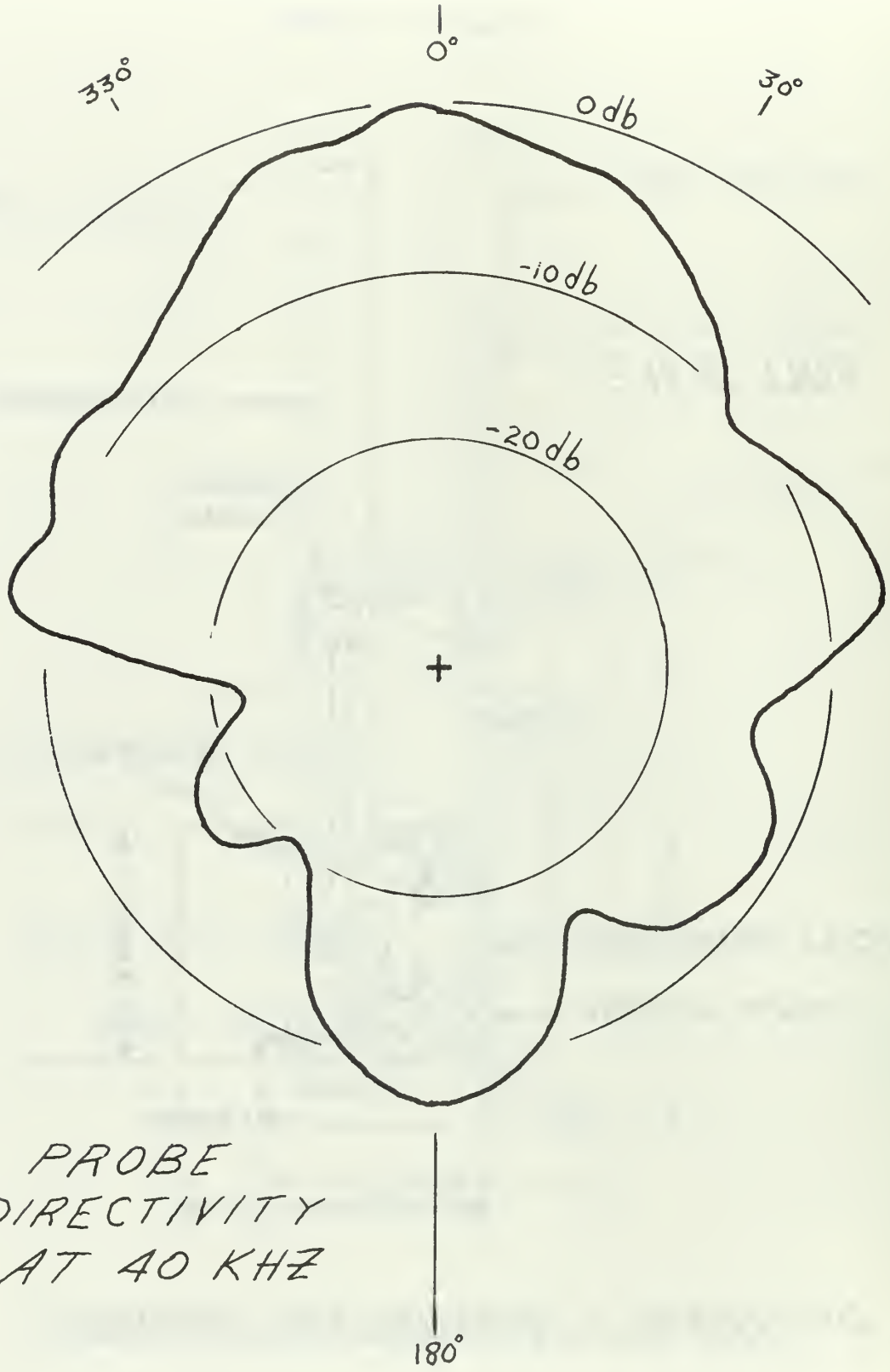

PROBE DIRECTIVITY AT 40 KHZ

FIGURE 3

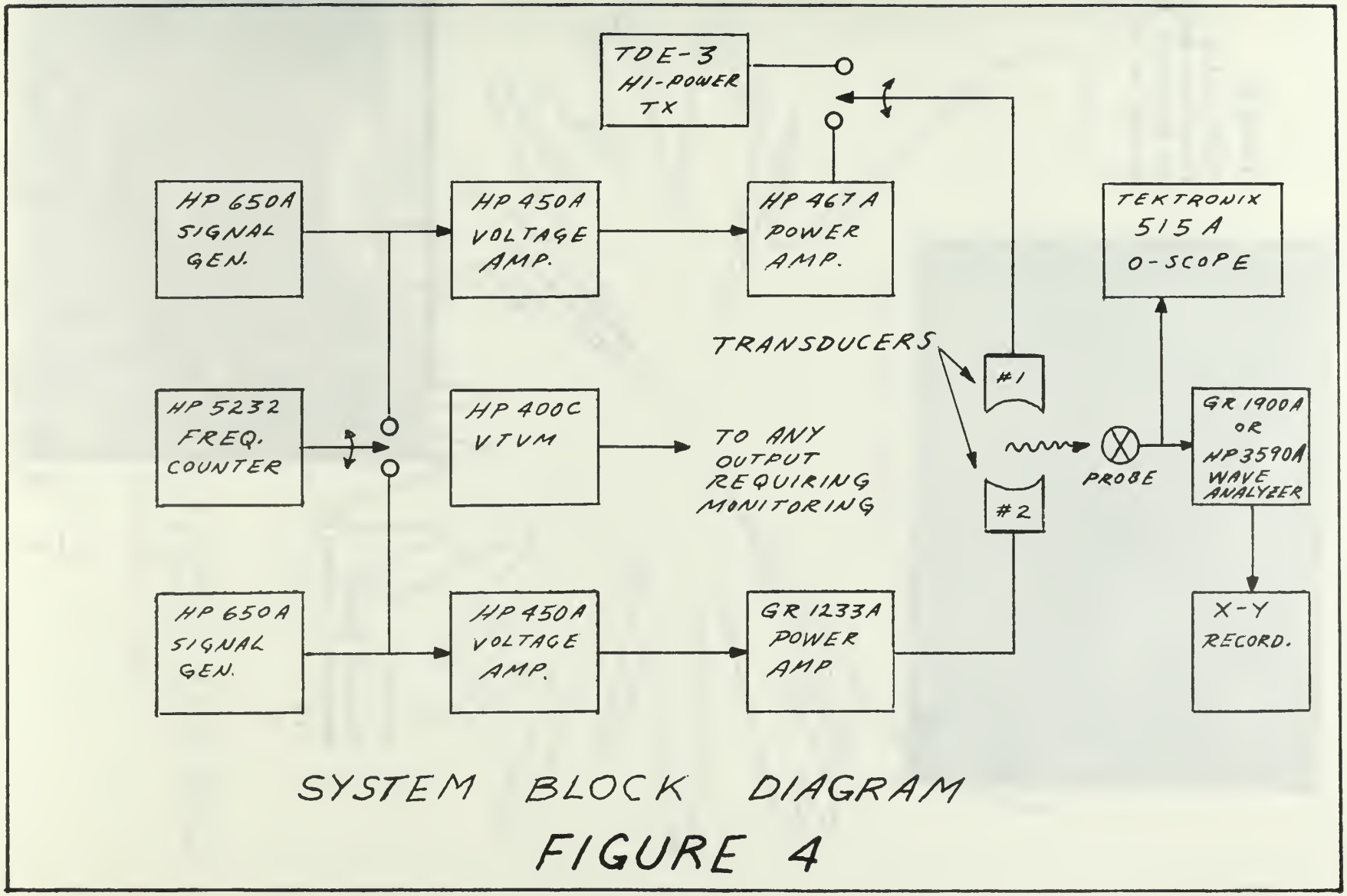

SYSTEM BLOCK DIAGRAM

FIGURE 4

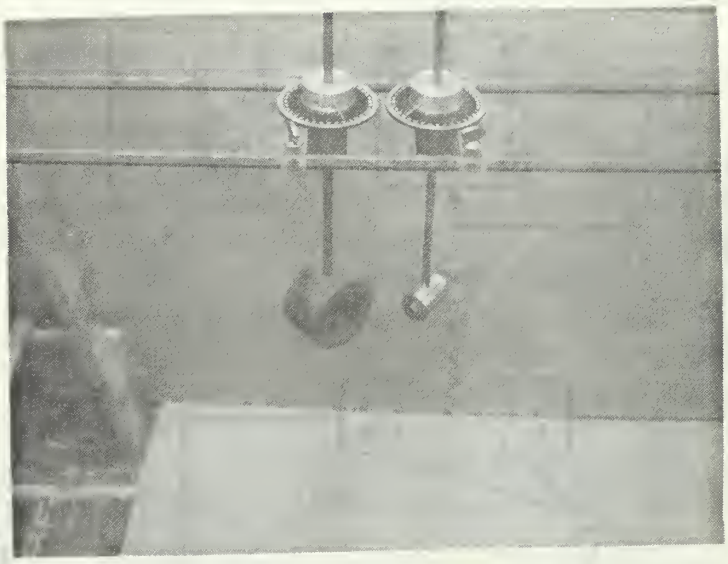

Figure 5

One Focusing Transducer and the Low Frequency Probe Mounted on the Rail

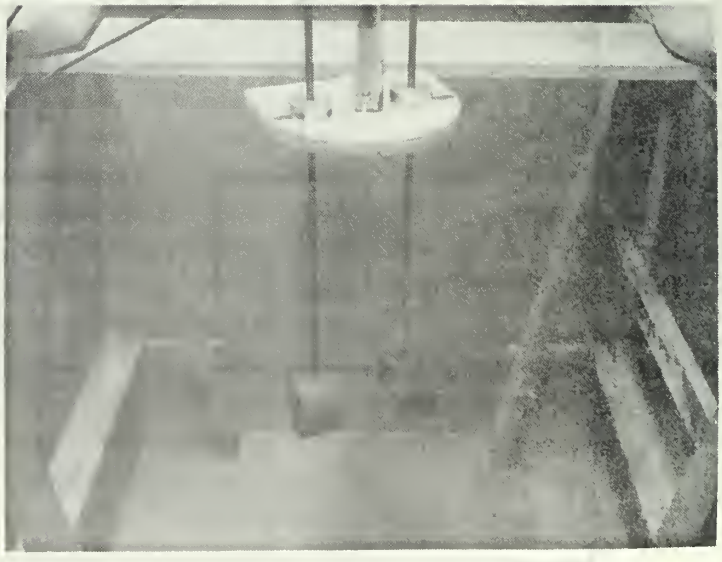

Figure 6

Focused System Mounted in Rotation Jig

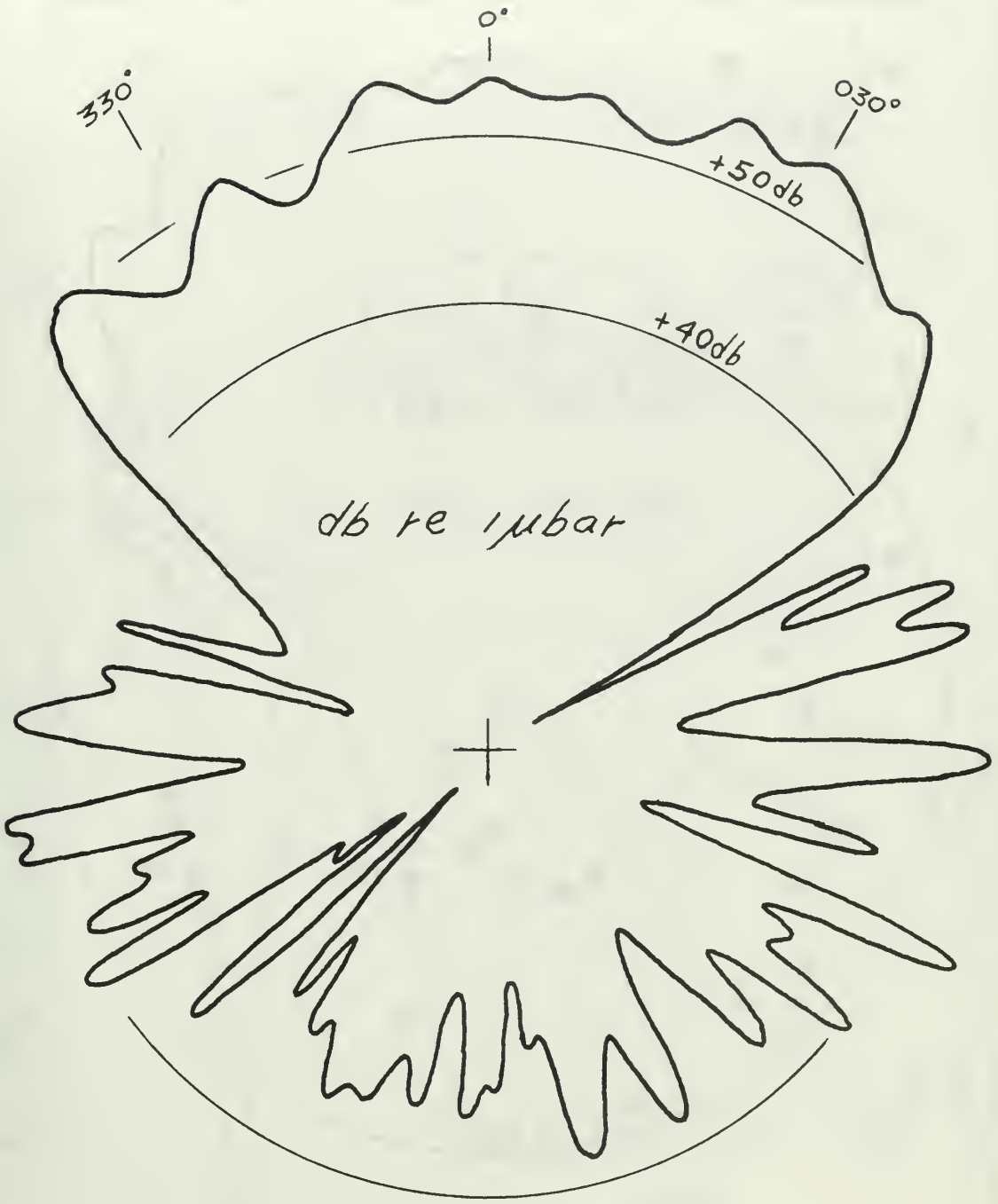

HEMISPHERE'S RADIATION AT 5.4 CM
15V P-P AT 383 KHZ

FIGURE 7

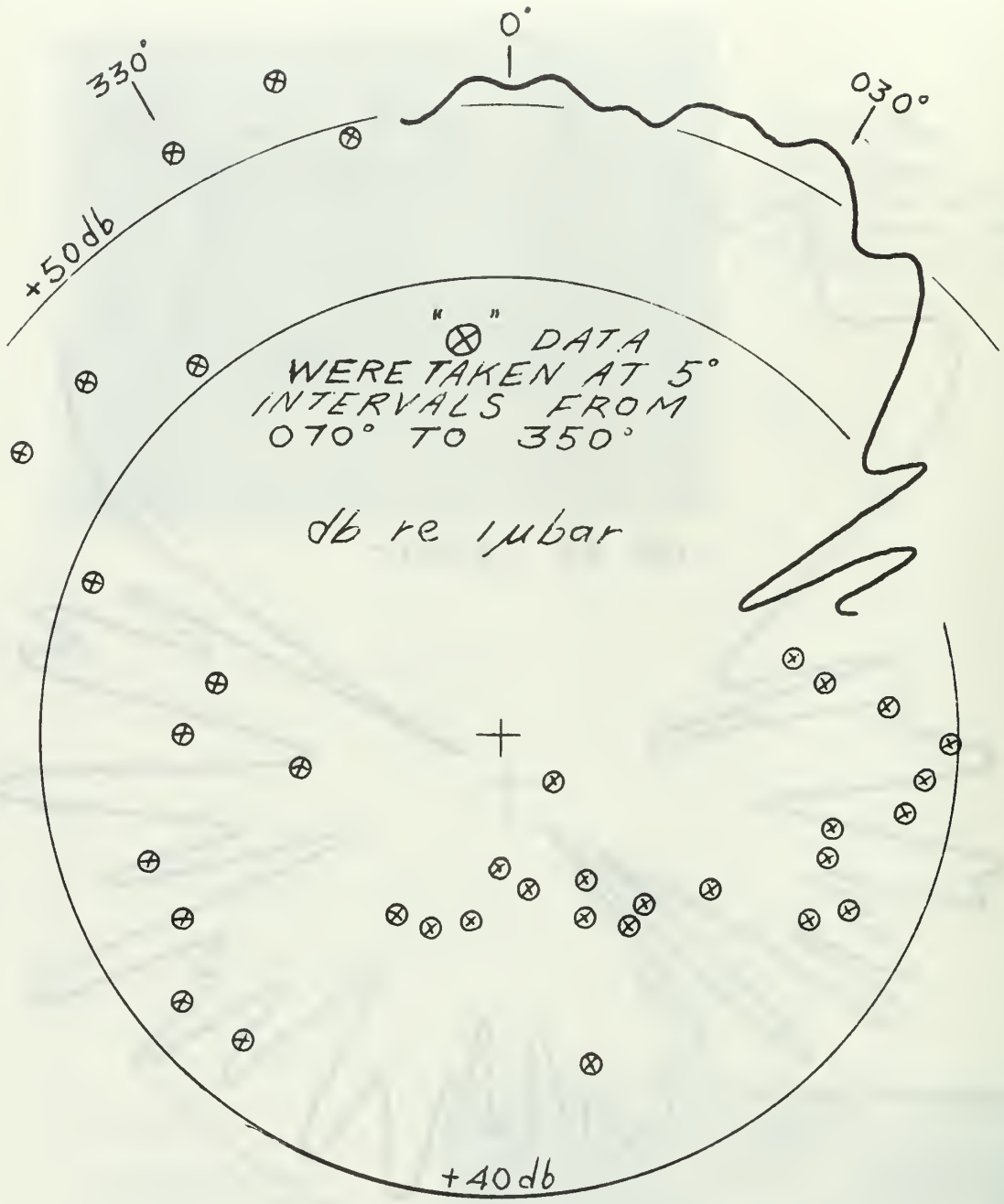

HEMISPHERE'S RADIATION AT 10.8CM
15V P-P AT 343KHZ

FIGURE 8

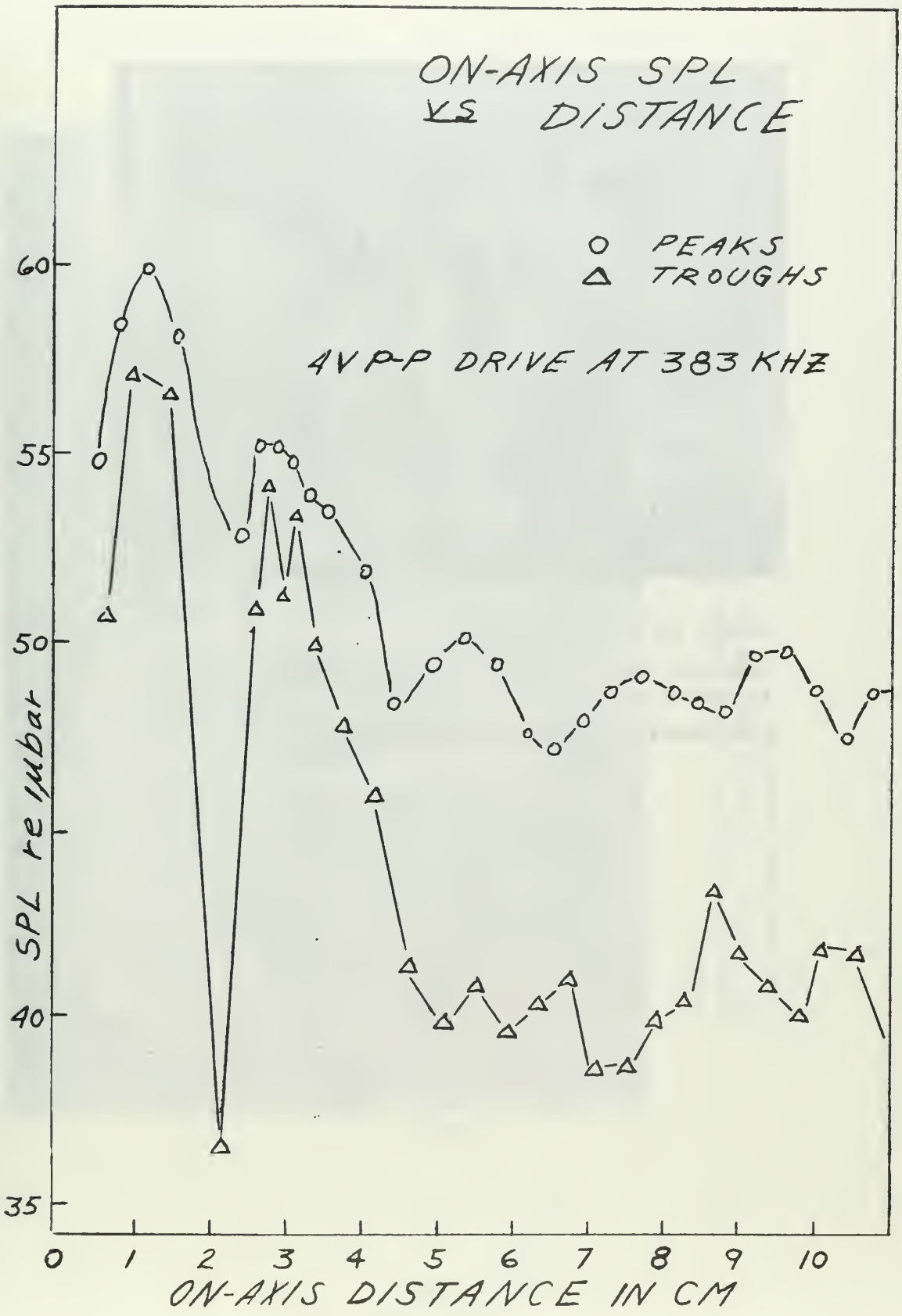
ON-AXIS SPL
VS DISTANCE
PEAKS
TROUGHS
4V P-P DRIVE AT 383 KHZ
60
55
50
40
35
SPL re 1μbar
0
1
2
3
4
5
6
7
8
9
10
ON-AXIS DISTANCE IN CM

FIGURE 9

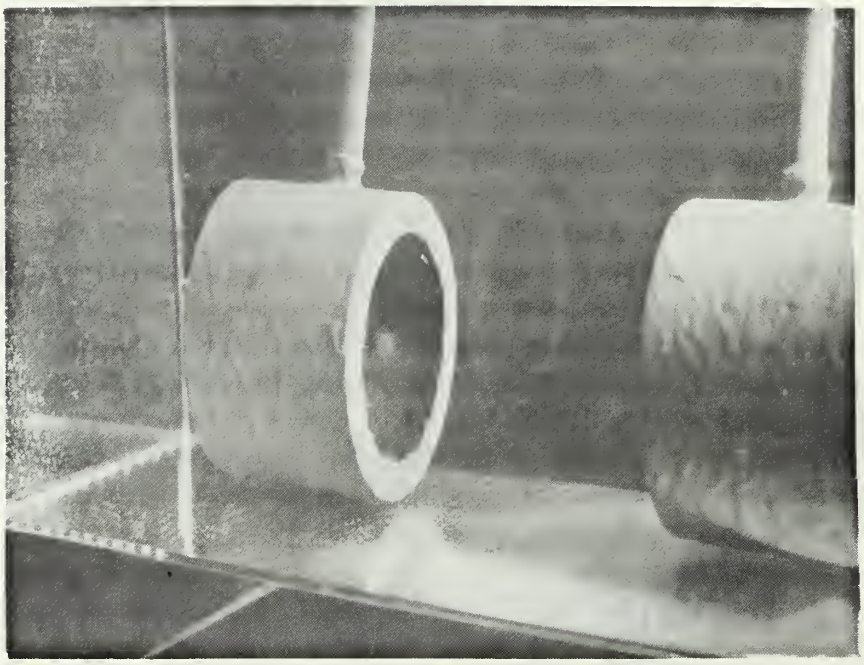

Figure 10

Transient cavitation in the Focal Region. Drive is 170V p-p at 343 kHz

Transducer at Right was Open Circuited

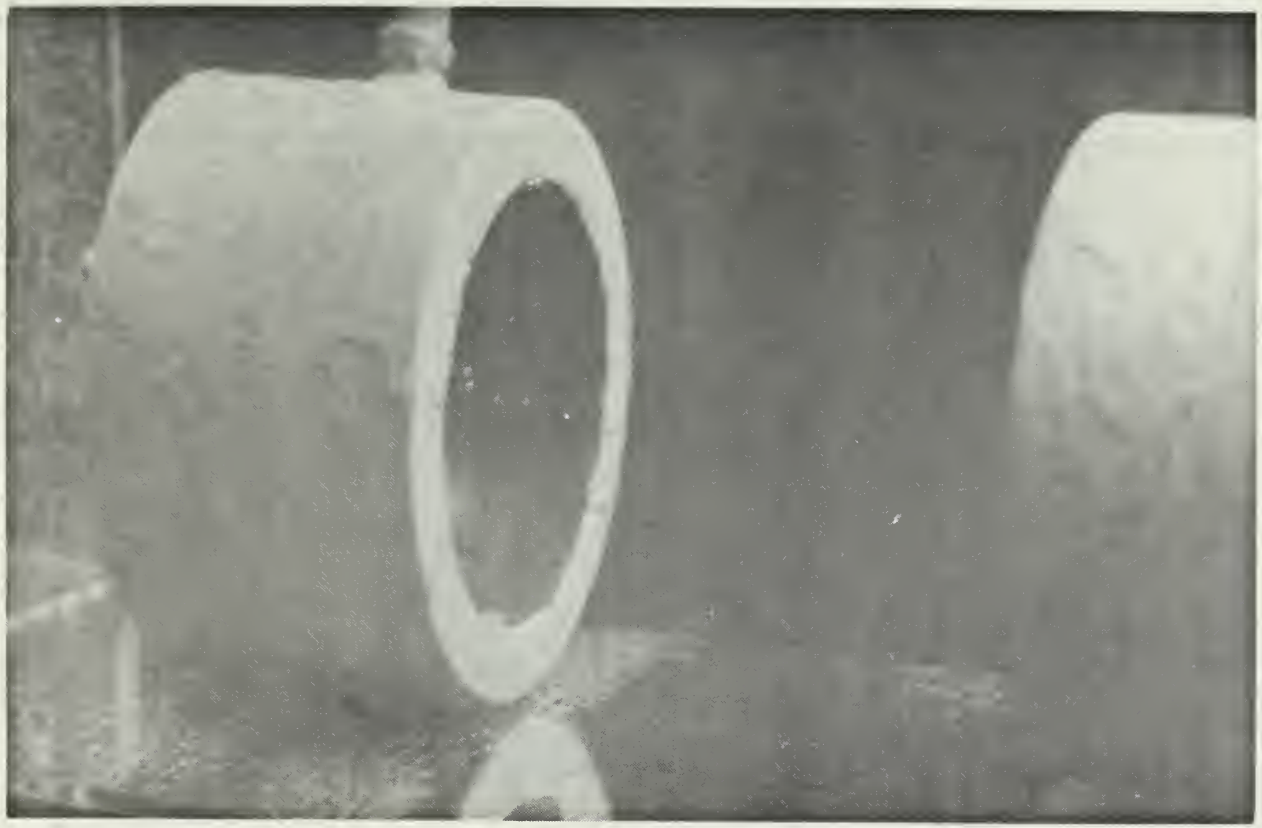

Figure 11
Cavitation Bubbles in Focal Region One Minute After Voltage was Applied. Drive is 30V p-p at 383 kHz. Transducer at Right was Open Circuited.

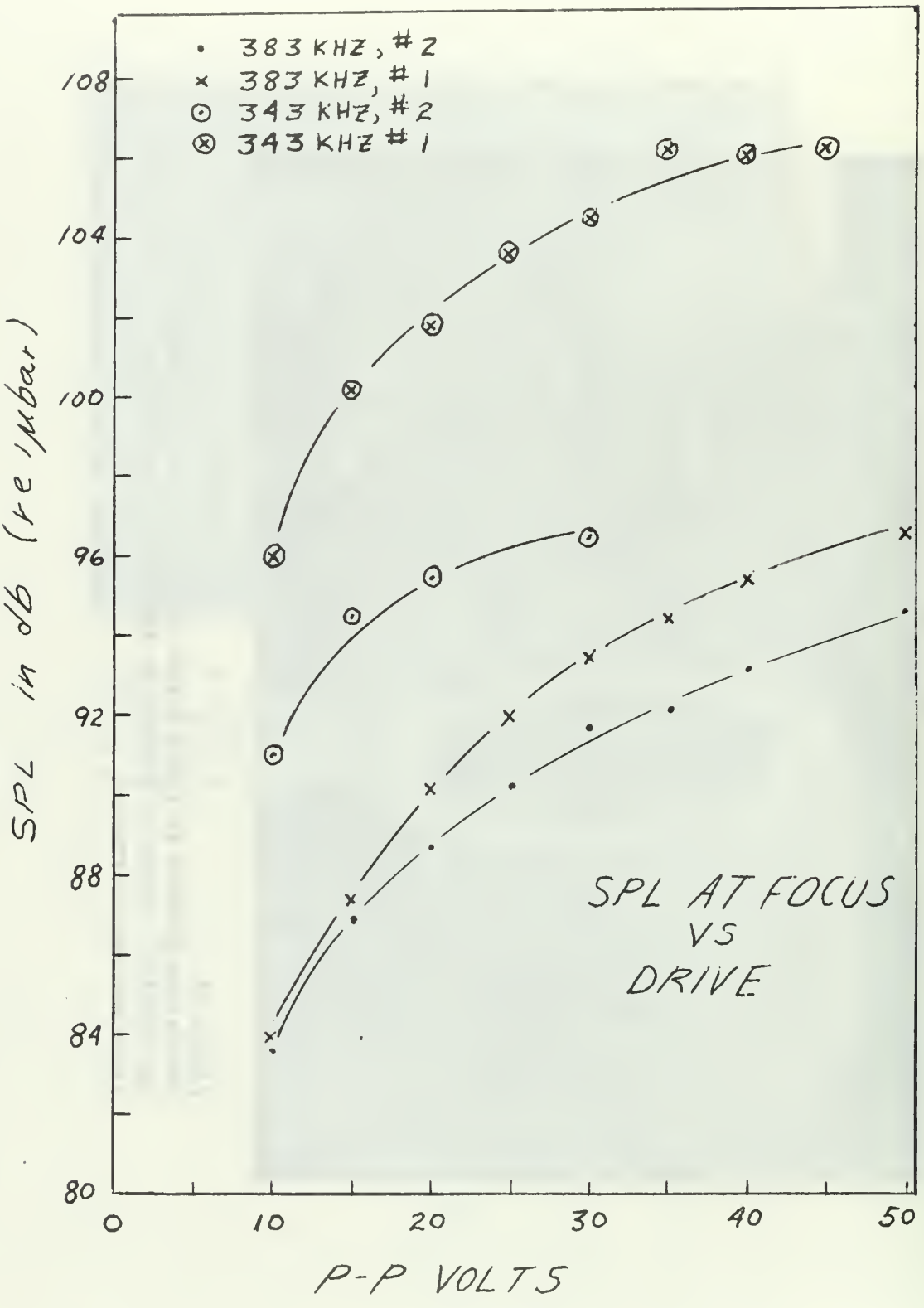
383 KHZ, #2
383 KHZ, #1
343 KHZ, #2
343 KHZ #1
108
104
100
96
92
88
84
80
SPL in dB (re 1μbar)
0
10
20
30
40
50
P-P VOLTS
SPL AT FOCUS
VS
DRIVE

FIGURE 12

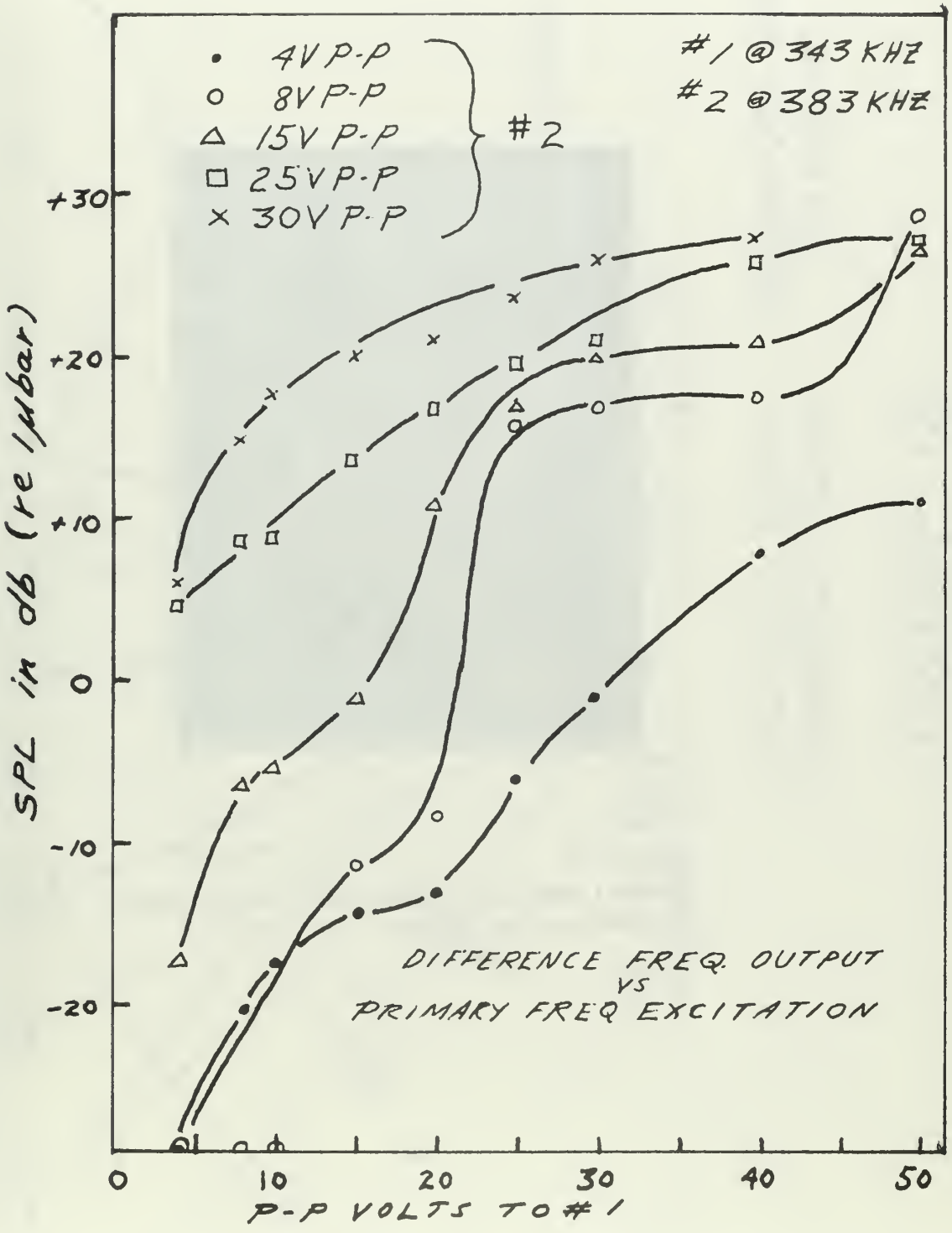
4V P-P
8V P-P
15V P-P
25V P-P
30V P-P
#2
#1 @ 343 KHZ
#2 @ 383 KHZ
+30
+20
+10
0
-10
-20
SPL in db (re 1/μbar)
DIFFERENCE FREQ. OUTPUT
VS
PRIMARY FREQ EXCITATION
0
10
20
30
40
50
P-P VOLTS TO #1

FIGURE 13

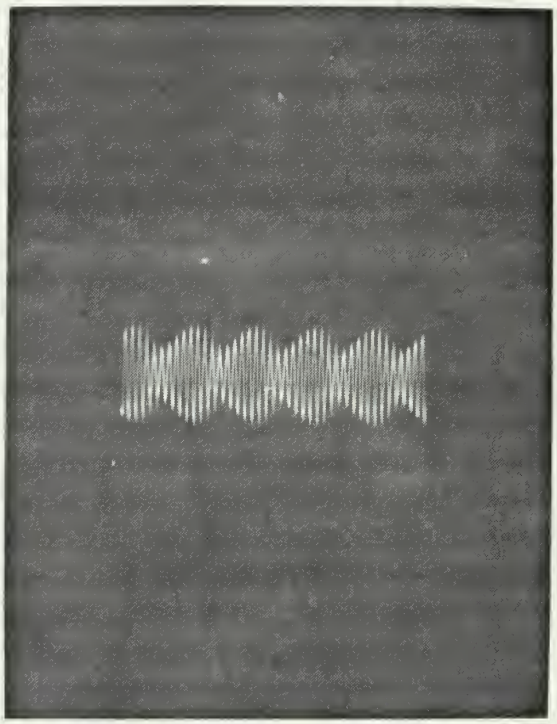

Figure 14

Typical Received Signal Prior to Filtering
The Carrier is 363 kHz

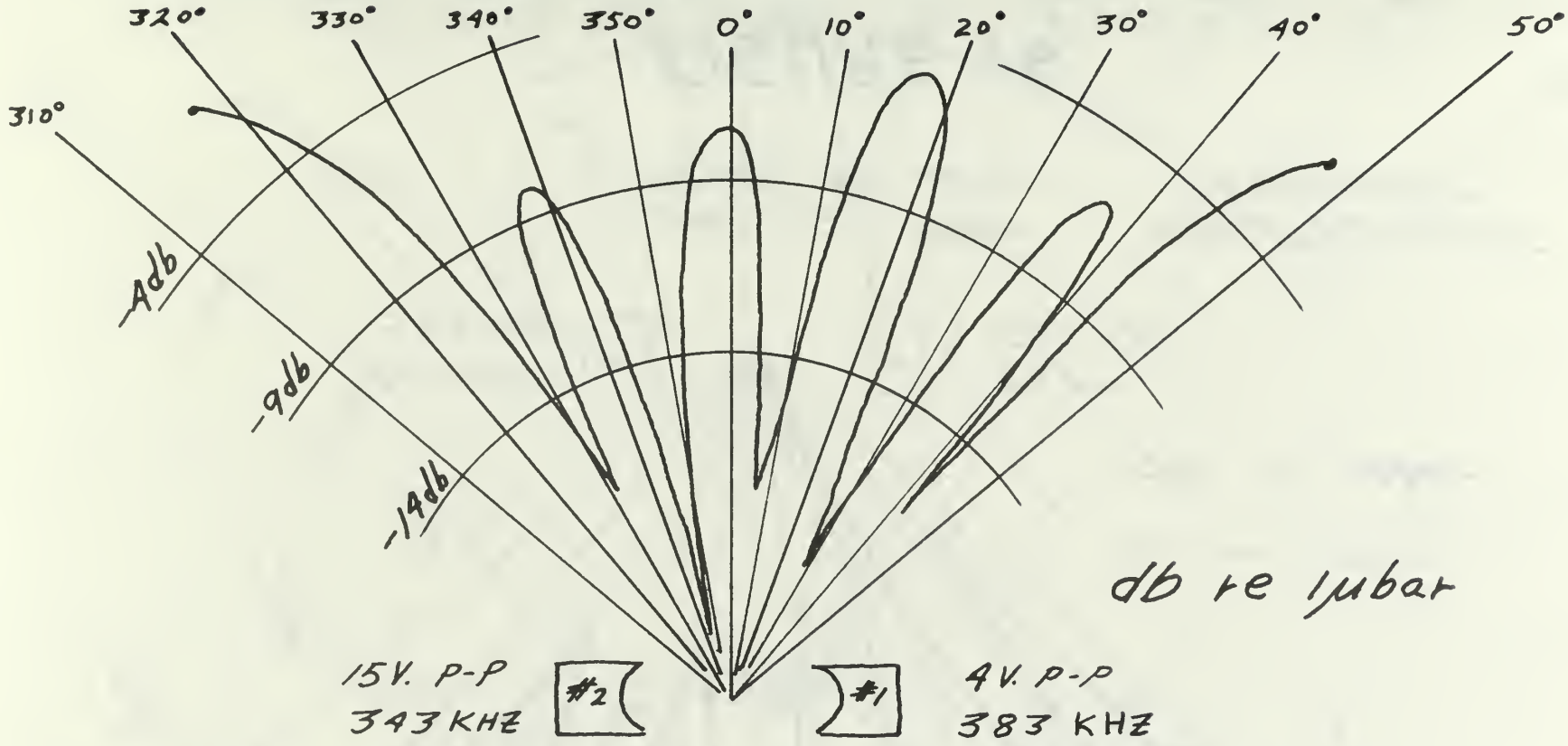
320°
330°
340°
350°
0°
10°
20°
30°
40°
50°
310°
4db
-9db
-19db
db re 1μbar
15V. P-P
343 KHZ
#2
#1
4V. P-P
383 KHZ
SPACING = 7.0 CM
PROBE AT 66 CM
RADIATED DIFF. FREQUENCY

FIGURE 15

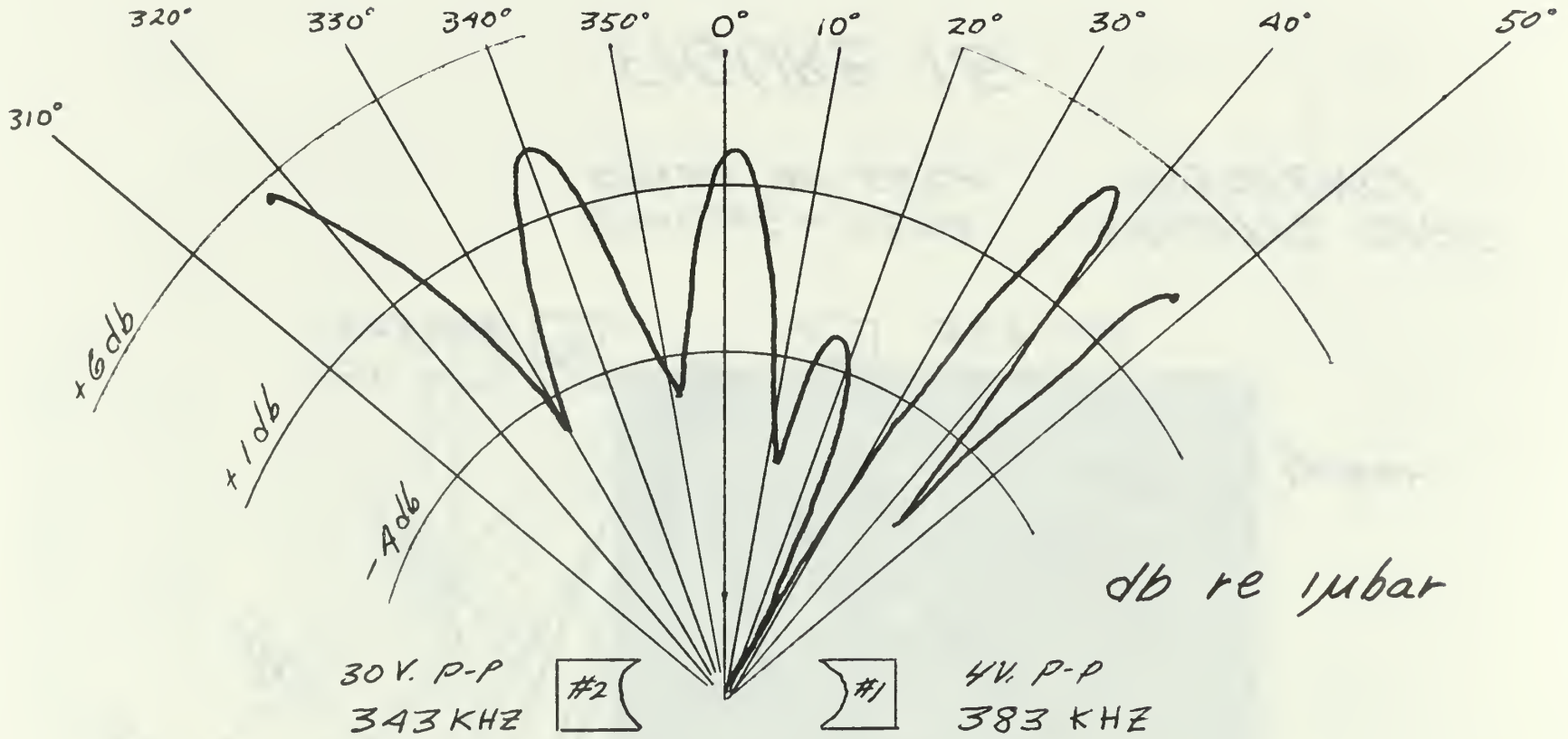
320°
330°
340°
350°
0°
10°
20°
30°
40°
50°
310°
+6db
+1db
-4db
db re 1μbar
30 V. P-P
343 KHZ
#2
#1
4V. P-P
383 KHZ
SPACING = 7.0CM
PROBE AT 66CM
RADIATED DIFF. FREQUENCY

FIGURE 16

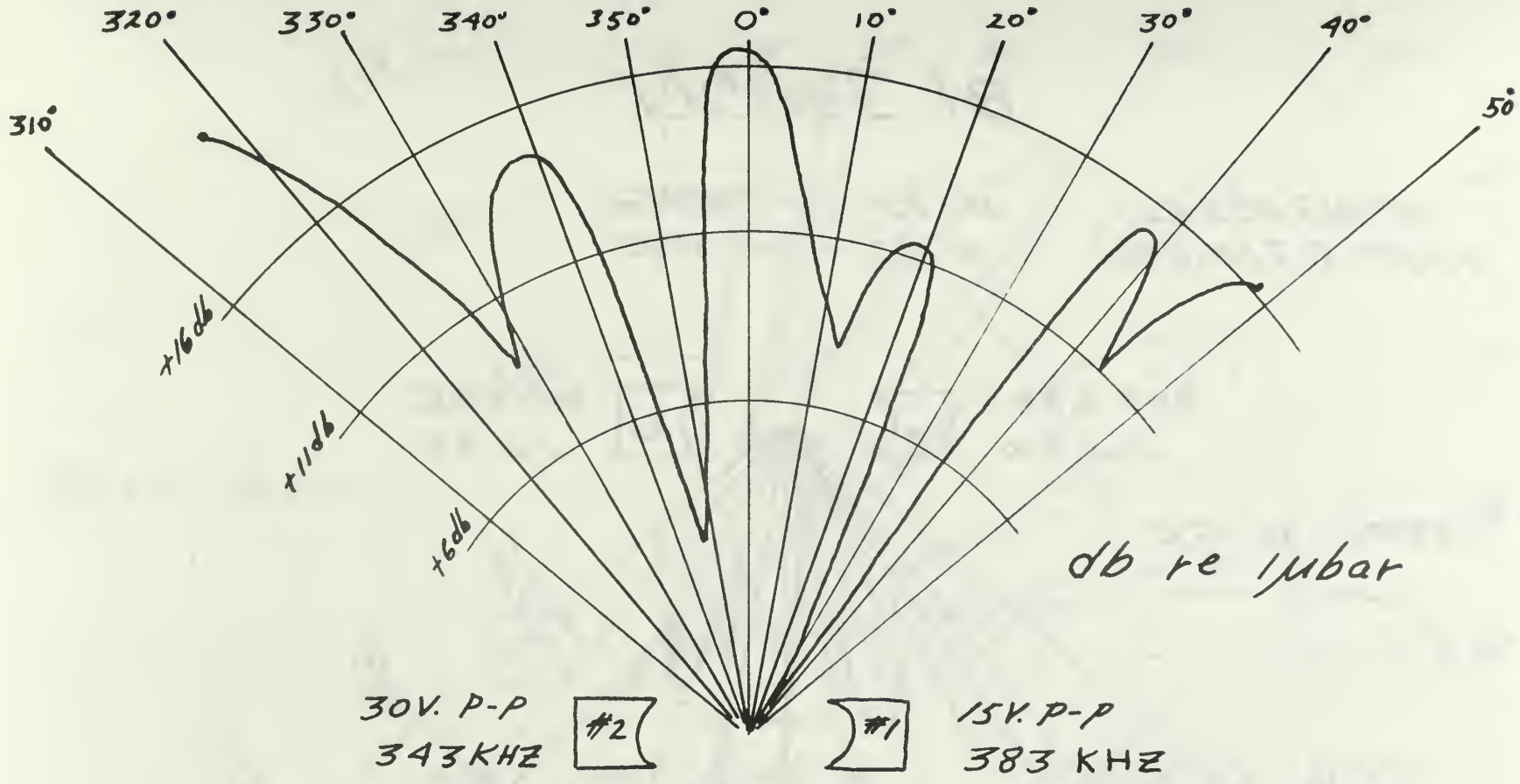

FIGURE 17

RADIATED DIFF. FREQUENCY

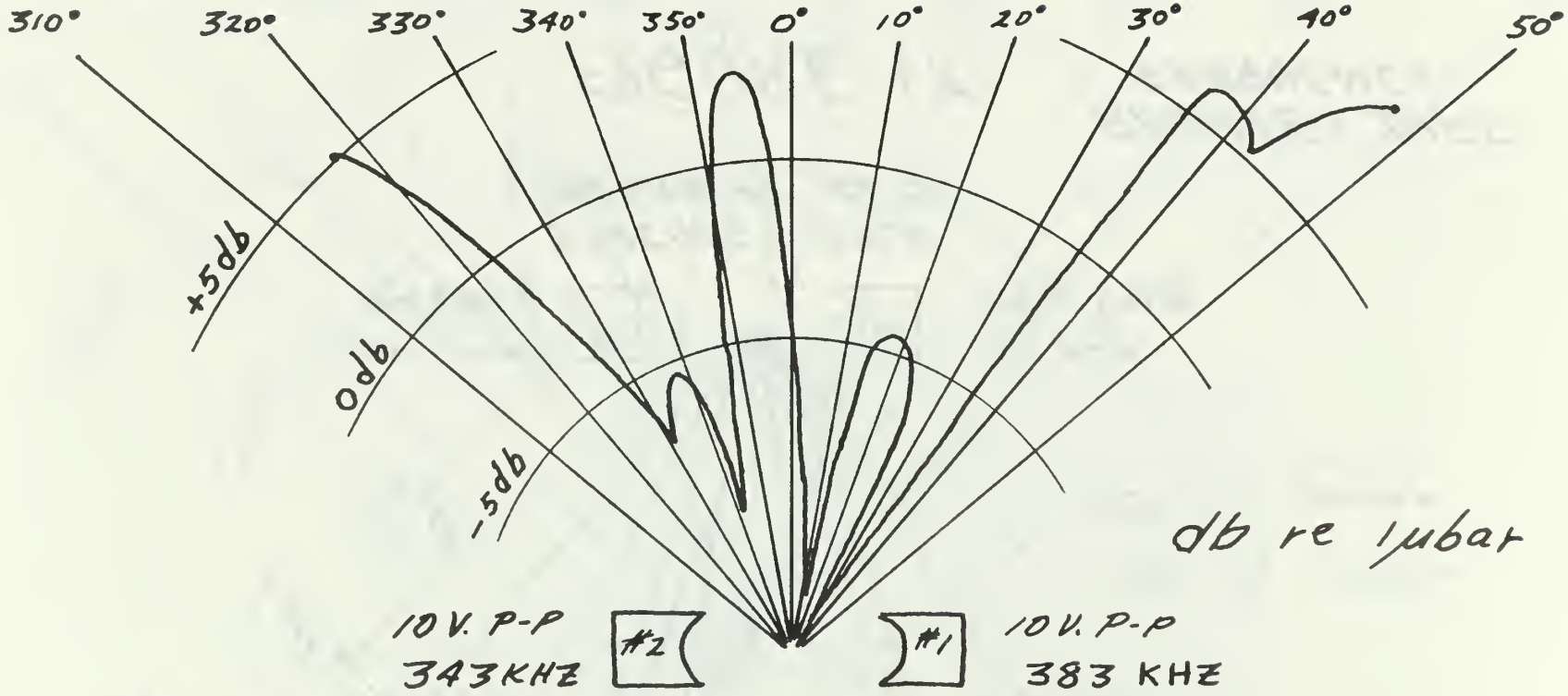
310°
320°
330°
340°
350°
0°
10°
20°
30°
40°
50°
+5db
0db
-5db
db re 1μbar
10 V. P-P
343 KHZ
#2
#1
10 V. P-P
383 KHZ
SPACING = 7.0CM
PROBE AT 66 CM
RADIATED DIFF. FREQUENCY

FIGURE 18

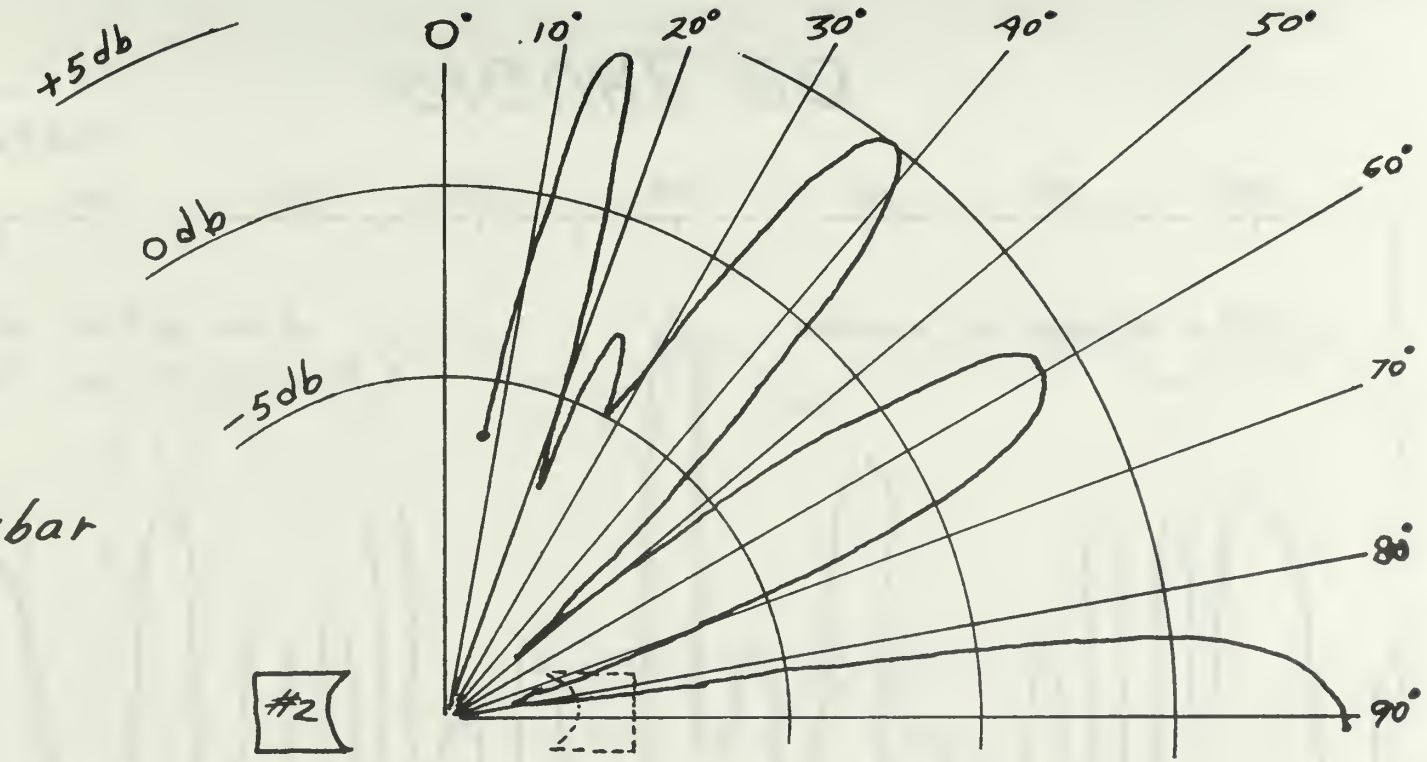

db re 1μbar

SAME CONDITIONS AS FOR FIGURE 18

RADIATED DIFF. FREQUENCY

FIGURE 19

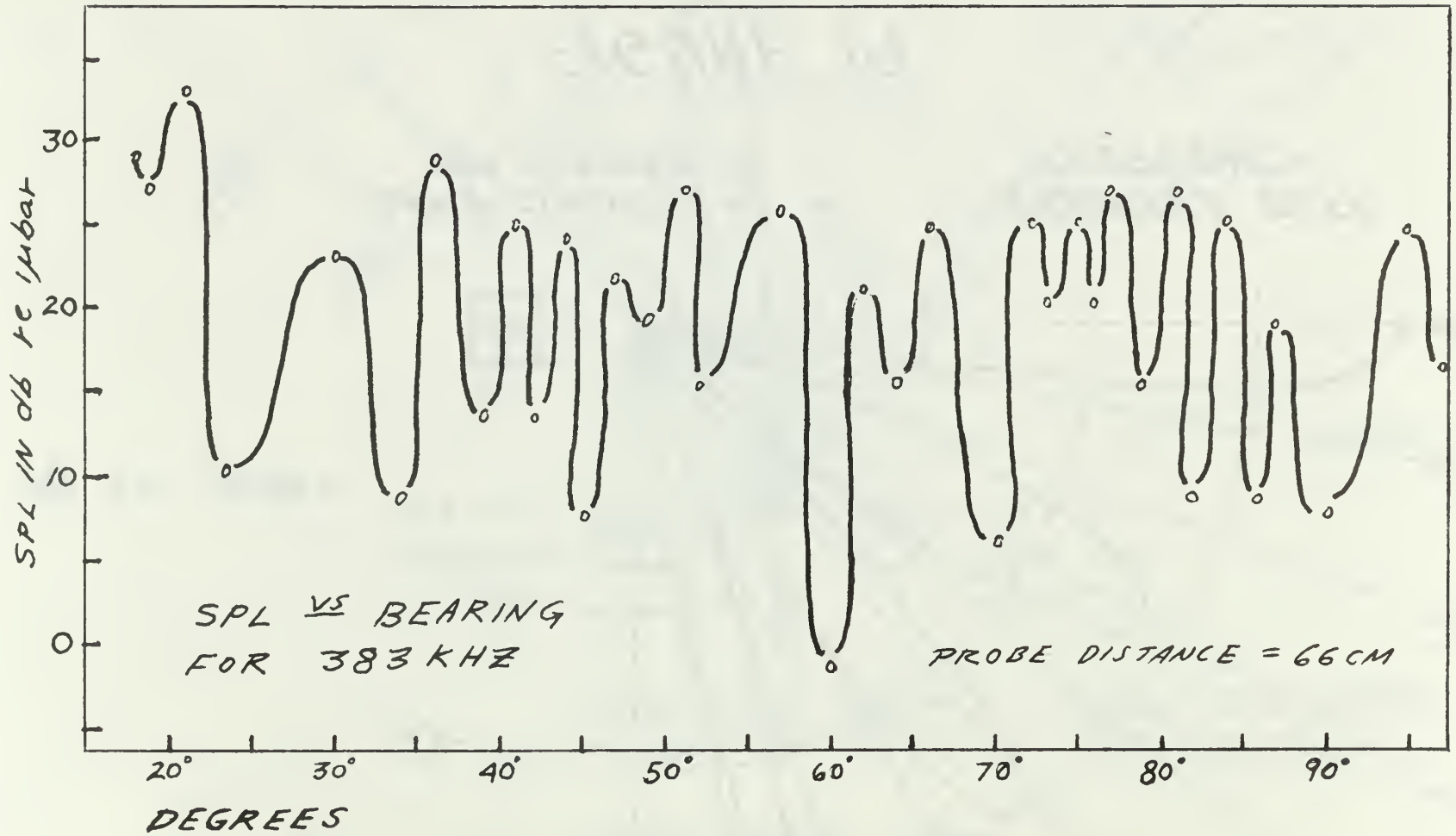
SPL IN dB re 1μbar
30
20
10
0
SPL VS BEARING
FOR 383 KHZ
PROBE DISTANCE = 66 CM
20°
30°
40°
50°
60°
70°
80°
90°
DEGREES

FIGURE 20

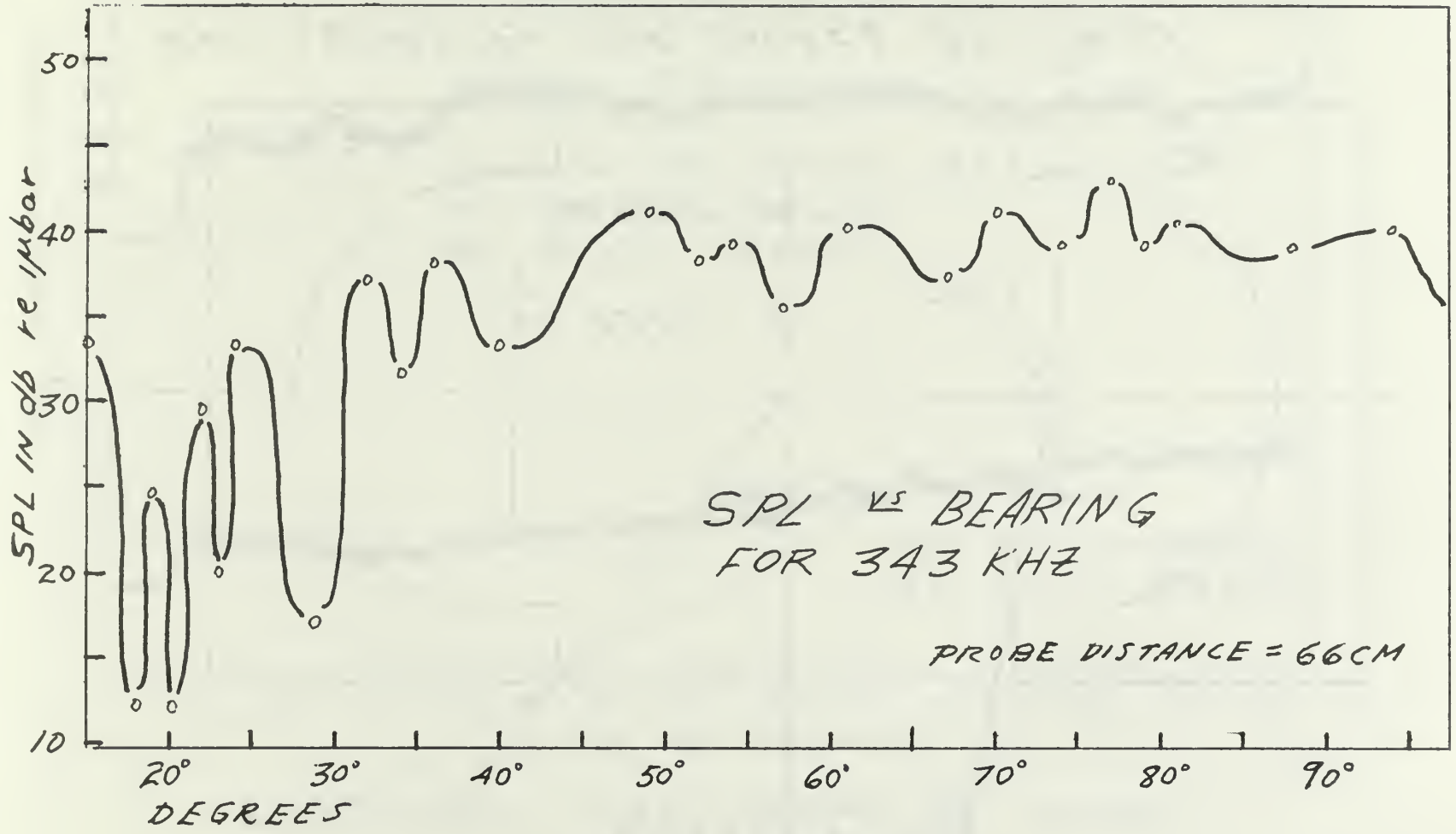
SPL IN db re 1μbar
50
40
30
20
10
20°
30°
40°
50°
60°
70°
80°
90°
DEGREES
SPL VS BEARING
FOR 343 KHZ
PROBE DISTANCE = 66CM

FIGURE 21

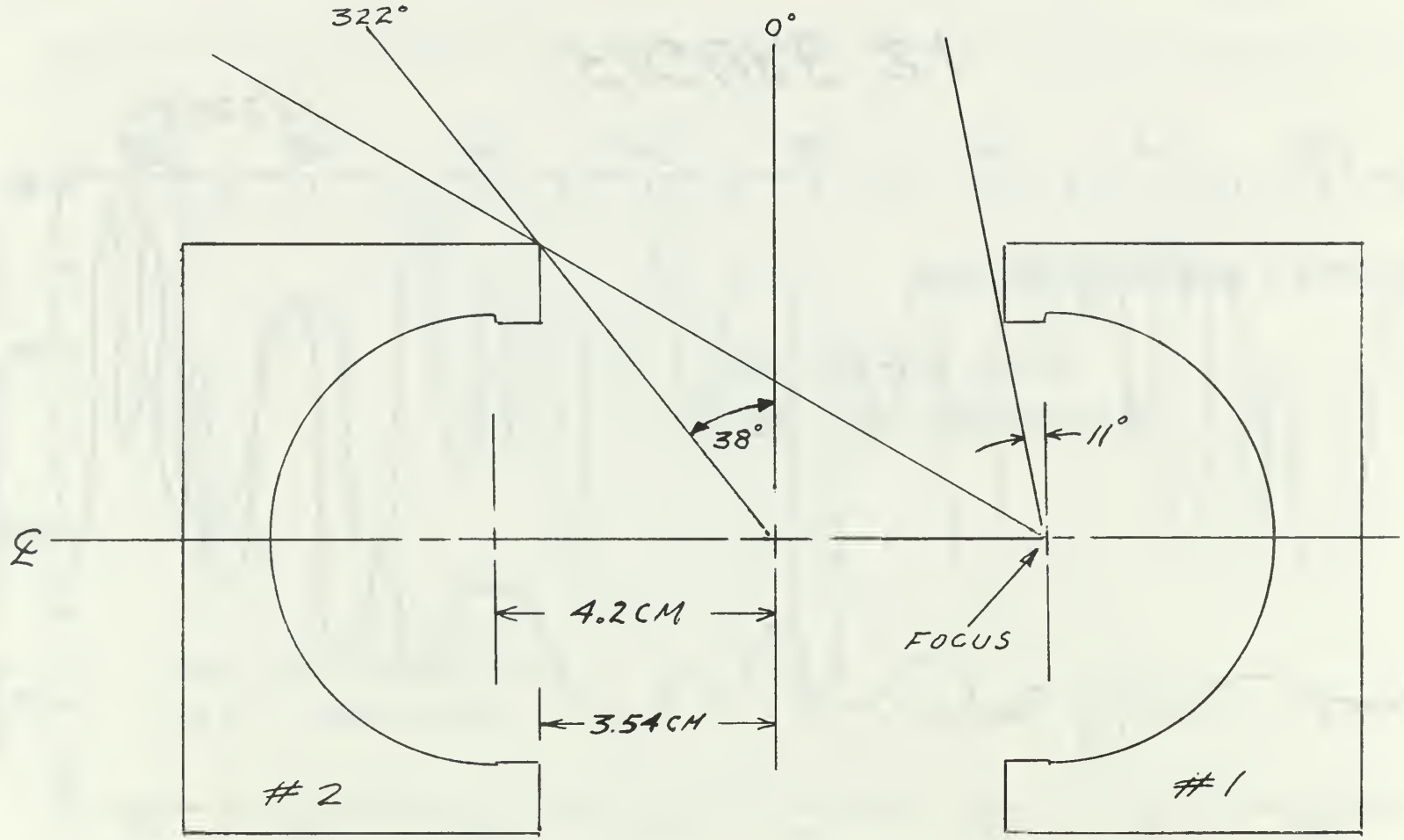

RAY GEOMETRY FOR SOURCE AT FOCUS

FIGURE 22

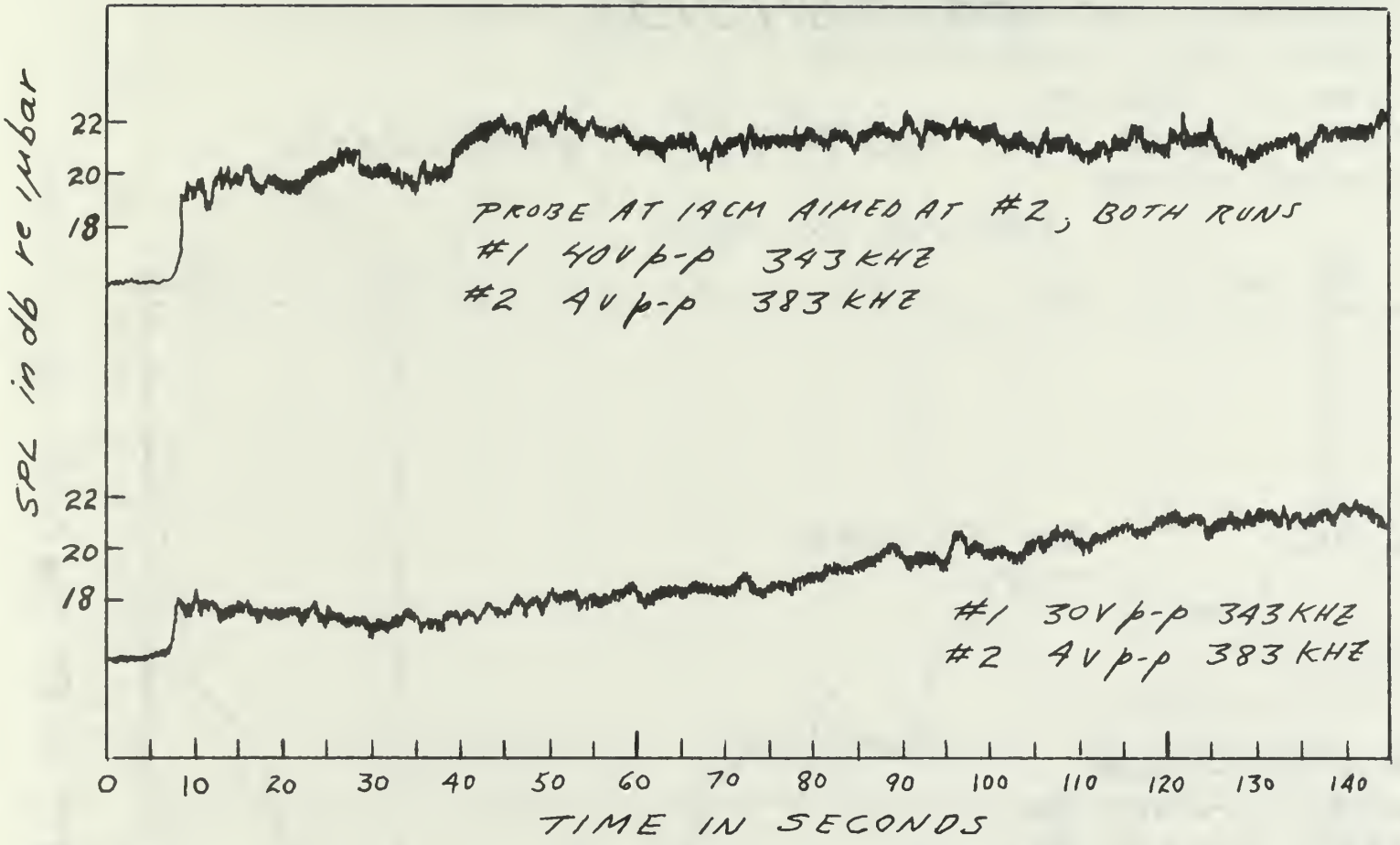

DIFFERENCE FREQUENCY VS TIME

FIGURE 23

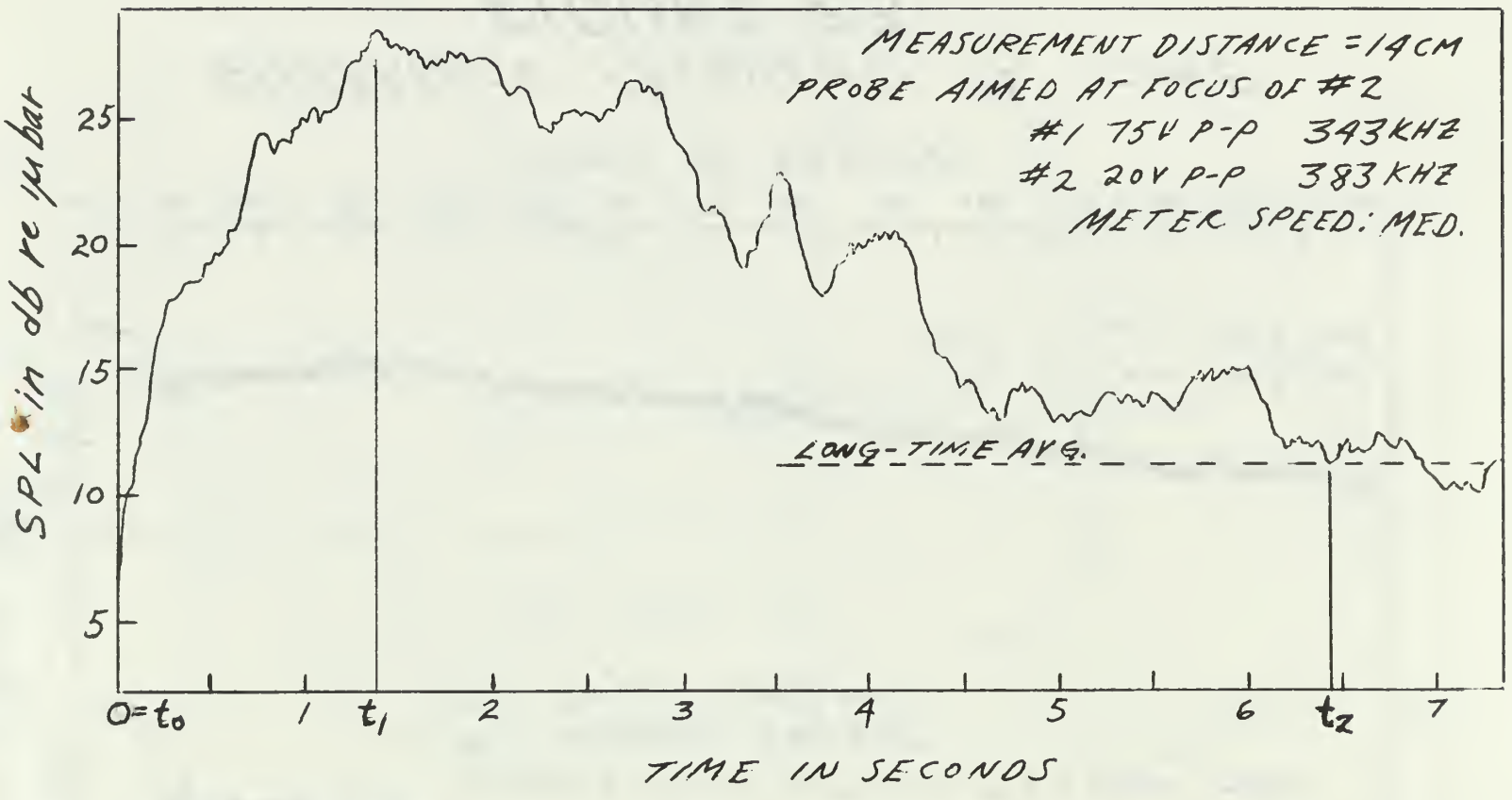

DIFFERENCE FREQUENCY VS TIME

FIGURE 24

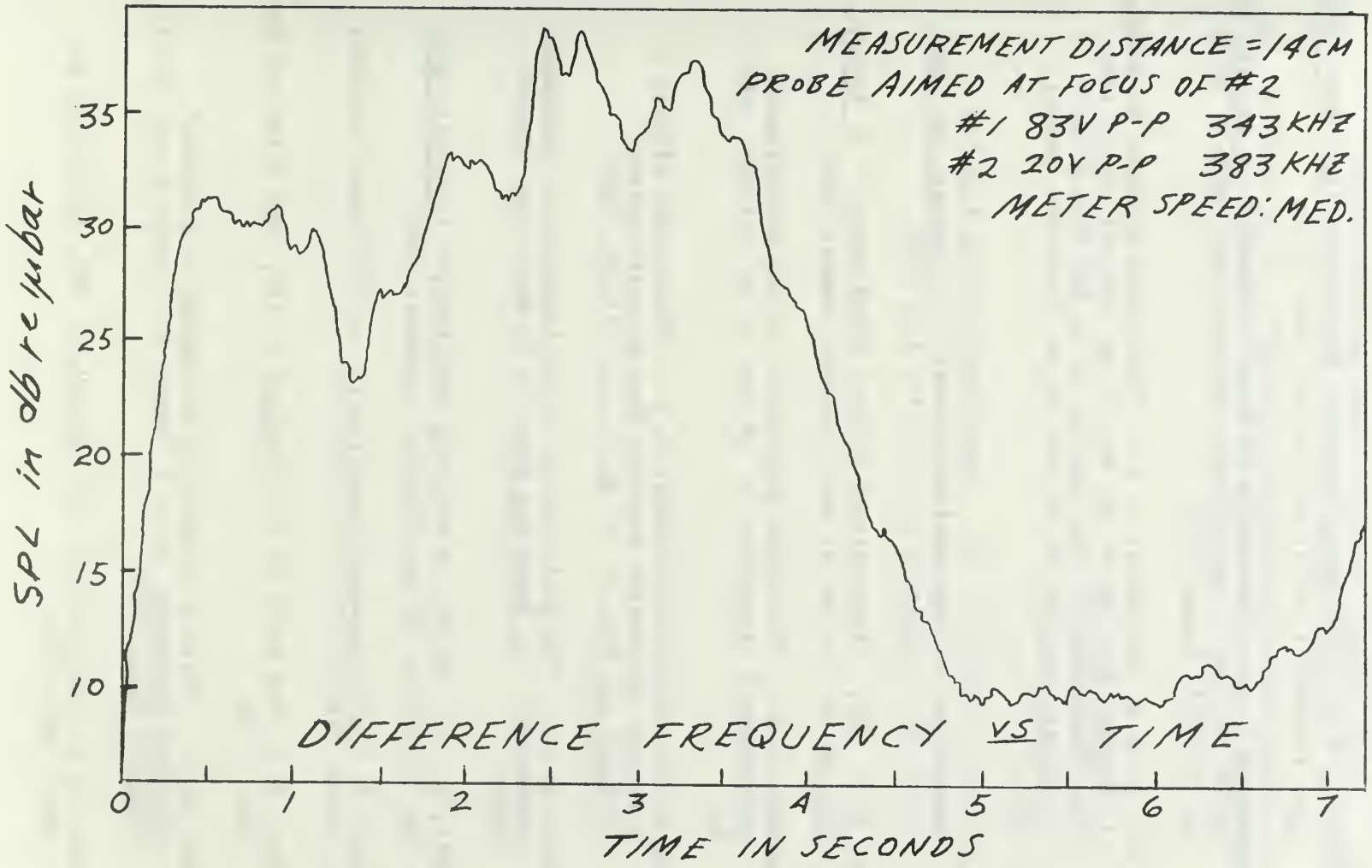
MEASUREMENT DISTANCE = 14CM
PROBE AIMED AT FOCUS OF #2
#1 83V P-P 343KHZ
#2 20V P-P 383KHZ
METER SPEED: MED.
SPL in db re μbar
35
30
25
20
15
10
DIFFERENCE FREQUENCY VS TIME
0
1
2
3
4
5
6
7
TIME IN SECONDS

FIGURE 25

BIBLIOGRAPHY

1. Lighthill, M. J., "On Sound Generated Aerodynamically," Proc. Royal Soc. (London),V. A211, pp. 564-587, Nov. 1951.

2. Westervelt, P. J., "Scattering of Sound by Sound," J. Acoust. Soc. Am. V. 29, No. 2, pp. 199-202, February 1957; also V. 29, No. 8, pp. 934-935, August 1957.

3. Bellin, J. L. S. and Beyer, R. T., "Scattering of Sound by Sound," J. Acoust. Soc. Am. V. 32, No. 3, pp. 339-341, March 1960. also "Experimental Investigation of an End-Fire Array," J. Acoust. Soc. Am. V. 34, No. 8, pp. 1051-1094, August, 1962.

4. Muir, T. G. and Blue, J. E., "Experiments on the Acoustic Modulation of Large-Amplitude Waves," J. Acoust. Soc. Am., V. 46, No. 1, part 2, pp. 227-232, July 1969.

5. Dean, W. L. III, "Interactions between Sound Waves," J. Acoust. Soc. Am.,V. 34, No. 8, pp. 1039-1044, August 1962.

6. Lauvstad, V. R., "Nonlinear Interaction of Two Monochromatic Soundwaves," Acoustica, V. 16, No. 4, pp. 191-217, 1965-66.

7. Dunn, D. J., Kuljis, M., Welsby, V. G., "Non-linear Effects in a Focused Underwater Standing Wave Acoustic System," J. Sound and Vib., V. 2, No. 4, pp. 471-476, 1965.

8. Tucker, D. G., "The Exploitation of Non-linearity in Underwater Acoustics," J. Sound and Vib., V. 2, No. 4, pp. 429-434, 1965.

9. O'Neil, H. T., "Theory of Focusing Radiators," J. Acoust. Soc. Am. V. 21, No. 5, pp. 516-526, September 1949.

10. Albers, V. M., Underwater Acoustics II, p. 279, Penn. State Univ. Press, 1965.

11. Hueter, T. F. and Bolt, R. H., Sonics, p. 116, John Wiley and Sons, Inc., 1955.

12. Flynn, H. G. "Physics of Acoustic Cavitation in Liquids," Physical Acoustics, by W. P. Mason, V. 1, part B, pp. 57-172, Academic Press, 1964.

13. Hueter, T. F., and Bolt, R. H., Sonics, p. 227, John Wiley and Sons, Inc., 1955.

14. De Santis, P., Sette, D., Wanderlingh, F., "Cavitation Detection: The Use of Subharmonics," J. Acoust. Soc. Am., V. 42, No. 2, pp. 514-516, July 1967.

15. Rozenberg, L. D., Sirotyuk, M. G., "Radiation of Sound in a Liquid with Cavitation Present," Soviet Phys. - Acoust., V. 6, No. 4, pp. 477-479, Apr-Jun 1961.

16. Berktay, H. O., "Possible Exploitation of Non-Linear Acoustics in Underwater Transmitting Applications," J. Sound and Vib. V. 2, No. 4, pp. 435-461, 1965.

INITIAL DISTRIBUTION LIST

		No. Copies
1.	Defense Documentation Center Cameron Station Alexandria, Virginia 22314	20
2.	Library, Code 0212 Naval Postgraduate School Monterey, California 93940	2
3.	Commander, Naval Ordnance Systems Command Department of the Navy Washington, D. C. 20360	1
4.	Commander, Naval Ship Systems Command Via Code 31, Code 2052 Department of the Navy Washington, D. C. 20360	1
5.	Assoc. Professor D. A. Stentz, Code 52Sz Department of Electrical Engineering Naval Postgraduate School Monterey, California 93940	1
6.	LT Kenneth F. Scigulinsky Sonar Programs Officer NAVSECNORDIV Norfolk, Virginia 23511	1
7.	Commander, Naval Undersea Research & Development Center San Diego, California 92132	1
8.	Naval Underwater Sound Laboratory Fort Trumbull New London, Connecticut 06320	1

DOCUMENT CONTROL DATA - R & D

(Security classification of title, body of abstract and indexing annotation must be entered when the overall report is classified)

1. ORIGINATING ACTIVITY *(Corporate author)*
Naval Postgraduate School
Monterey, California 93940

2a. REPORT SECURITY CLASSIFICATION
Unclassified

2b. GROUP

3. REPORT TITLE
Non-linear Effects in a Focused Underwater Acoustic System

4. DESCRIPTIVE NOTES *(Type of report and inclusive dates)*
Master's Thesis; December 1969

5. AUTHOR(S) *(First name, middle initial, last name)*
Kenneth Frank Scigulinsky

6. REPORT DATE	7a. TOTAL NO. OF PAGES	7b. NO. OF REFS
December 1969	56	16

8a. CONTRACT OR GRANT NO.	9a. ORIGINATOR'S REPORT NUMBER(S)
b. PROJECT NO.	
c.	9b. OTHER REPORT NO(S) *(Any other numbers that may be assigned this report)*
d.	

10. DISTRIBUTION STATEMENT
This document has been approved for public release and sale, its distribution is unlimited.

11. SUPPLEMENTARY NOTES	12. SPONSORING MILITARY ACTIVITY
	Naval Postgraduate School Monterey, California 93940

13. ABSTRACT

A focused system having non-coincident foci was used to study the phenomenon of non-linear mixing in water. Primary frequencies of 343 kHz and 383 kHz provided a scattered difference frequency of 40 kHz. Enhancement of the difference frequency signal at incipient cavitation was verified. A delay between energization of the system and signal enhancement was linked to the state of non-linearity of the medium and provided strong evidence for the existance of a virtual source at 40 kHz. Directivity measurements of the focused system at 40 kHz revealed a multilobed structure, but the presence of pseudosound degraded the measurements and attempts to correlate the lobe structure with a particular virtual source configuration were unsuccessful.

14 KEY WORDS	LINK A		LINK B		LINK C	
	ROLE	WT	ROLE	WT	ROLE	WT
Non-linear mixing						
Focused transducers						
Scattered difference frequency						
Virtual source						
Multilobed radiation pattern						